

AMERICAN UNIVERSITY OF BEIRUT

INSIGHTS INTO THE ROLE OF TUBULIN LIGASE-LIKE
FAMILY MEMBER 4 (TLL4) IN SELECTED BREAST CANCER
CELLS

by
ELVIRA ELIAS DIBO

A thesis
submitted in partial fulfillment of the requirements
for the degree of Master of Science
to the Department of Biology
of the Faculty of Arts and Sciences
at the American University of Beirut

Beirut, Lebanon
April, 2017

AMERICAN UNIVERSITY OF BEIRUT

INSIGHTS INTO THE ROLE OF TUBULIN TYROSINE
LIGASE-LIKE FAMILY MEMBER 4 (TLL4) IN SELECTED
BREAST CANCER CELL LINES

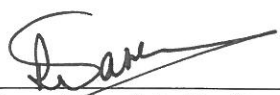
by
ELVIRA ELIAS DIBO

Approved by:



Dr. Diana Jaalouk, Assistant Professor
Biology

Advisor



Dr. Rihab Nasr, Associate Professor
Physiology

Co-Advisor



Dr. Rabih Talhouk, Professor
Biology

Member of Committee



Dr. Noël Ghanem, Assistant Professor
Biology

Member of Committee

Date of thesis/dissertation defense: [April 26, 2017]

AMERICAN UNIVERSITY OF BEIRUT

THESIS, DISSERTATION, PROJECT RELEASE FORM

Student Name:

_____ Dibo _____ Elvira _____ Elias _____
Last First Middle

Master's Thesis Master's Project Doctoral
Dissertation

I authorize the American University of Beirut to: (a) reproduce hard or electronic copies of my thesis, dissertation, or project; (b) include such copies in the archives and digital repositories of the University; and (c) make freely available such copies to third parties for research or educational purposes.

I authorize the American University of Beirut, to: (a) reproduce hard or electronic copies of it; (b) include such copies in the archives and digital repositories of the University; and (c) make freely available such copies to third parties for research or educational purposes
after : **One ---- year from the date of submission of my thesis, dissertation, or project.**
Two ---- years from the date of submission of my thesis, dissertation, or project.
Three ---- years from the date of submission of my thesis, dissertation, or project.

Signature

Date

ACKNOWLEDGEMENTS

“My soul magnifies the LORD” Luke 1:46

I am very grateful for the help and care Dr. Diana Jaalouk presented. She answered all my questions, was very patient and led me to the right path of knowledge. Dr. Rihab Nasr, was a very supportive collaborator of the project and believer of our research. She was ready to offer help and guidance when needed. I would like to thank her and my thesis committee members, Dr. Rabih Talhouk and Dr. Noel Ghanem, for not only serving on my thesis committee but also offering vital advice for the continuance of the project.

I would like to recognize Dr. Talhouk’s, Dr. Nasr’s and Dr. Ghanem’s lab members for presenting material as well as assistance when looked-for.

I acknowledge the awesome work of Abbas Ghaddar and his help in generating results. Despite his minimal experience in the lab, he was able to general reliable results and data that added flavor to this thesis.

I want to show deep gratitude for the DJ lab members for making this experience special. I want to thank Hind Zahr for the training and advice she generously gave throughout the spent in the lab. I would also like to thank Dima Diab El Harakeh for training me on different techniques and offering swift help when needed. I would like to thank Sara Assi for presenting moral and technical support at every stage. Moreover, I appreciate Ingrid Hajj for her reinforcement and amazing support. Last but not least, I want to thank Ranim Daw, my friend throughout the journey, for being a loyal and trustworthy acquaintance.

I want to deeply thank my soulmate, Rawad, for lifting me up and being there on the good and bad days. He taught me to appreciate the gift of learning and always pursue knowledge. I present deep appreciation for my family members for always pushing me towards improvement and perfection.

AN ABSTRACT OF THE THESIS OF

Elvira Elias Dibo for Master of Science
Major: Biology

Title: Insights into the Role of Tubulin Tyrosine Ligase-Like Family Member 4 (TTLL4) in Selected Breast Cancer Cell Lines

Tubulin Tyrosine Ligase-Like family member 4 (TTLL4) is one of a family of proteins which share a Tubulin Tyrosine Ligase (TTL) domain. TTLL4 functions in polyglutamylating numerous substrates, mainly β -tubulin. It is located in different cell compartments including the cytoskeleton where it is able to interact with tubulin permitting its branching and elongation. TTLL4 was shown to be overexpressed in various types of cancer; however, its expression and putative role in breast cancer has not been fully inspected. After looking into the Cancer Cell Line Encyclopedia (CCLE) database, TTLL4 mRNA expression levels vary across a panel of 58 breast cancer cell lines, but are consistently higher than TTLL4 expression in normal tissue. TTLL4 promotes the initiation of β -tubulin polyglutamylation. Therefore, Paclitaxel (Taxol®), the β -tubulin targeting chemotherapeutic drug, may have an effect on TTLL4 or vice versa. As such we hypothesize TTLL4 expression is upregulated in breast cancer than in normal tissue and that its expression levels impact cellular sensitivity to the tubulin-targeting chemotherapy drug Paclitaxel. It is also possible that TTLL4 expression and/or function are altered in response to treatment with Paclitaxel. For the purpose of this study, we examined the change of TTLL4 expression at the transcript and protein levels under baseline conditions and after Paclitaxel treatment. We assessed the transcript expression of TTLL4 by Real-time PCR, where RNA was extracted from MCF-7 and MDA-MB-231 cells under baseline conditions. This expression was also determined post treatment with Paclitaxel for 8hrs, 2hrs and 30 mins at the following concentrations: 0nM, 14nM, 55nM and 220nM (IC_{50}) for MCF-7 cells, and 0nM, 20nM, 80nM and 320nM (IC_{50}) for MDA-MB-231 cells. Under baseline conditions, MCF-7 cells showed higher *TTLL4* expression than MDA-MB-231 cells. Upon treatment with Paclitaxel, both cell lines showed no significant change in *TTLL4* expression. To examine the protein expression of TTLL4, we used a variety of methods including Immunofluorescence, Western blot and ELISA with the Paclitaxel treatment time points being 24hrs, 12 hrs and 6hrs. Under baseline conditions, TTLL4 was more expressed in MCF-7 than MDA-MB-231 cells when assessed by Immunofluorescence. Both cell lines showed increased TTLL4 expression upon treatment with Paclitaxel with the increase of time and concentration. However, the difference in TTLL4 expression was undecipherable by Western blotting because of the various TTLL4 isoforms (10 isoforms) and its high level of phosphorylation. Moreover, the complexity of

TLL4 did not allow us to determine its protein via ELISA as well. Ongoing work and future directions will focus on looking at the expression of TLL4 in MCF10A, the less invasive cell line, and compare it to the results of MCF-7 and MDA-MB-231 cell lines. Additionally, further optimization for western blots for TLL4 is needed in addition to checking for other ways to determine TLL4 protein expression. Furthermore, knocking down TLL4 and overexpressing it would give us a better idea about the essentiality of TLL4 in breast cancer survival, invasiveness and response to therapy. In addition the effect of Paclitaxel on TLL4's enzymatic activity is yet to be determined.

CONTENTS

ACKNOWLEDGEMENTS.....	v
ABSTRACT.....	vi
LIST OF ILLUSTRATIONS.....	xii
LIST OF TABLES.....	xiii
LIST OF ABBREVIATIONS.....	xiv

Chapter

I. LITERATURE REVIEW	1
A. Mammary Gland	1
1. Overview.....	1
2. Development and gene expression.....	1
B. Breast Cancer.....	3
1. Overview.....	3
2. Breast Cancer Subtypes.....	4
C. Breast Cancer Treatment.....	6
1. Treatment Options.....	6
2. Chemotherapy.....	6
D. Paclitaxel.....	7
1. Overview.....	7
2. Mechanism of Action of Paclitaxel.....	7
3. Resistance Mechanisms of Paclitaxel.....	8

a.	Overview.....	8
b.	Tubulin Alterations Conferring Paclitaxel Resistance.....	9
E.	Tubulin Tyrosine Ligase-Like (TTLL) Proteins	10
1.	Overview.....	10
2.	Functions of TTLL Proteins.....	11
3.	Polyglutamylation.....	11
a.	Overview.....	11
b.	Polyglutamylation on Tubulin.....	12
4.	Specific Activities of TTLL Proteins.....	12
F.	TTLL4.....	13
1.	Overview.....	13
2.	The Different TTLL4 Isoforms.....	13
3.	Role of TTLL4 in Cancer.....	15
G.	Gap in Knowledge, Study Rationale and Hypothesis.....	15
H.	Objective of the Study and Specific Aims.....	17
I.	Significance of the Study.....	18
 II. MATERIALS AND METHODS		19
A.	Maintenance of Cells in Tissue Culture.....	19
1.	MCF-7.....	19
2.	MDA-MB-231.....	19
3.	Cell Count	19
B.	RNA Extraction.....	20
1.	Baseline Conditions.....	20
2.	Paclitaxel Treatment.....	20
3.	Verification via RNeasy.....	22
C.	Reverse Transcription.....	22

D. Real-Time PCR.....	23
E. Protein Extraction, SDS-PAGE & Western Blot Analysis.....	24
1. Protein Extraction.....	24
a. Baseline Conditions.....	24
b. Paclitaxel Treatment.....	25
2. Sample Protein Quantification.....	25
a. SDS-PAGE: : Sodium Dodecyl Sulfate-Polyacrylamide Gel Electrophoresis.....	26
b. Casting & Running the Gel.....	26
c. Preparing & Loading the Samples.....	27
d. Protein Transfer from Gel to Blot.....	28
e. Membrane Blocking, Washing & Antibody Incubations.....	29
f. X-ray Film Imaging of Western Blots.....	30
g. Membrane Stripping & Re-probing.....	30
F. Immunofluorescence Staining.....	31
1. Baseline Conditions.....	31
2. Paclitaxel Treatment.....	32
G. Microscopic Imaging.....	33
H. Enzyme Linked Immunosorbent Assay (ELISA) Optimization...	33
I. Statistical Analysis.....	35
III. RESULTS.....	36
A. Optimization of Paclitaxel Treatment.....	36
B. Real-time PCR.....	37

1. Under baseline conditions, <i>TLL4</i> normalized to <i>GAPDH</i> is more expressed in MCF-7 than in MDA-MB-231 cells. This increase is statistically significant	37
2. In MCF-7 cells, <i>TLL4</i> normalized to <i>GAPDH</i> insignificantly varies in transcript levels upon treatment with Paclitaxel (14nM, 55nM and 220nM) for 30mins, 2hrs and 8hrs with respect to their untreated controls.	39
3. In MDA-MB-231 cells, <i>TLL4</i> normalized to <i>GAPDH</i> insignificantly differs in transcript levels upon treatment with Paclitaxel (20nM, 80nM and 320nM) for 30mins, 2hrs and 8hrs with respect to their untreated controls.....	40
4. <i>TLL4</i> and <i>GAPDH</i> Cq values are not significantly altered in TRIzol RNA extraction method in comparison to RNeasy extraction	41
C. <i>TLL4</i> Protein Expression	42
1. <i>TLL4</i> protein is differentially expressed in MCF7 and MDA-MB-231 cells under baseline conditions by immunofluorescence staining.....	42
2. <i>TLL4</i> protein is distinctly expressed in MCF-7 cell line post-Paclitaxel treatment by immunofluorescence staining.....	44
3. <i>TLL4</i> protein is distinctly expressed in MDA-MB-231 cell line post-Paclitaxel treatment by immunofluorescence staining	46
4. <i>TLL4</i> protein in MCF-7 and MDA-MB-231 cell lines under baseline conditions by Western Blot.....	48
5. <i>TLL4</i> protein in MCF-7 cells post-Paclitaxel treatment by Western Blot.....	49
6. <i>TLL4</i> protein in wild type MEFs under baseline conditions by Western Blot.....	51
7. Troubleshooting for <i>TLL4</i> protein expression in MCF-7 cells by ELISA.....	52
 IV. DISCUSSION.....	55
 V. REFERENCES.....	60

ILLUSTRATIONS

Figure	Page
1. Stages of Development of the Mammary Glands	3
2. Mechanism of action of Paclitaxel.....	8
3. Phosphorylation Sites on human TTLL4.....	15
4. Counts of MCF-7 and MDA-MB-231 cells for Paclitaxel treatment optimization.....	37
5. Mean fold change in <i>TTLL4</i> transcript expression in MCF-7 and MDA-MB-231 cells at baseline conditions.....	38
6. Mean fold change in <i>TTLL4</i> transcript expression in MCF-7 post-Paclitaxel treatment.....	40
7. Mean fold change in <i>TTLL4</i> transcript expression in MDA-MB-231 cells post-Paclitaxel treatment.....	41
8. Mean fold change in <i>TTLL4</i> transcript expression in MDA-MB-231 under baseline conditions by TRIZOL versus RNeasy RNA extraction.....	42
9. Immunofluorescence staining of TTLL4 protein in MCF-7 and MDA-MB-231 cells under baseline conditions.....	43
10. Immunofluorescence staining of TTLL4 protein in MCF-7 cells after Paclitaxel treatment (0nM, 14nM, 22nM and 220nM).....	45
11. Immunofluorescence staining of TTLL4 protein in MDA-MB-231 cells after Paclitaxel treatment (0nM, 20nM, 80nM and 320nM).....	47
12. Western Blot of TTLL4 protein expression in MCF-7 and MDA-MB-231 cells under baseline conditions.....	49
13. Western Blot of TTLL4 protein expression in MCF-7 after treatment with Paclitaxel.....	50
14. Western Blot of TTLL4 protein expression in wild-type MEFs under baseline conditions.....	52
15. Curve of the O.D. readouts at 450nm for the human anti-TTLL4 ELISA protein standards of concentrations 0.625, 1.25, 2.5, 5, 10 and 20 ng/ml.....	53

TABLES

Table	Page
1. The Different Isoforms of TTLL4.....	14
2. A list of the forward and reverse primers used to quantify select mechanosensitive genes by Real-Time PCR.....	24
3. O.D. readouts of the ELISA troubleshooting attempts to detect and quantify TTLL4 in Paclitaxel treated MCF-7 cells.....	54

ABBREVIATIONS

%	Percent
/	Per
°C	Degrees Celsius
α	Alpha
β	Beta
Aa	Amino acid
ATP	Adenosine Triphosphate
Bcl-2	B-cell lymphoma 2
Bp	Base pair
BSA	Bovine Serum Albumin
DAPI	4',6-Diamidino-2-Phenylindole
DCIS	Ductal Carcinoma in situ
ddH ₂ O	Deionized distilled water
DMSO	Dimethyl sufoxide
DNA	Deoxyribonucleic Acid
ECM	Extracellular Matric
EGF	Epidermal Growth Factor
ER	Estrogen receptor
et al.	et alii (and others)
FBS	Fetal bovine serum
FGF	Fibroblast Growth Factor
g	Grams
g/ mol	Grams per mol
GAPDH	Glyceraldehyde 3-phosphate dehydrogenase
GTP	Guanosine Triphosphate
HER	Human Epidermal Growth Factor Receptor
HGF	Hepatocyte Growth Factor
HRP	Horseradish peroxidase
Hrs	Hours
Hz	Hertz
IDC	Invasive Ductal Carcinoma
IGF1	Insulin-like Growth Factor 1
ILC	Invasive Lobular Carcinoma
In Situ	On Site
Kb	Kilo base pairs
KDa	Kilo Dalton
Ki67	Cellular Marker for Proliferation
LCIS	Lobular Carcinoma in situ
MAP	Microtubule Associated Protein

MCF-7	Michigan Cancer Foundation cells number 7
MDA-MB-231	Monroe Dunaway Anderson Metastatic Breast cancer cells number 231
MEF	Mouse Embryonic Fibroblast
Mg	Milligram
min	Minute
ml	Milliliter
mm	Millimeters
mRNA	Messenger Ribonucleic Acid
NaOH	Sodium Hydroxide
NF- κ B	Nuclear Factor Kappa-light-chain-enhancer of activated B cells
nm	Nano Meter
nM	Nano Molar
O.D.	Optical Density
P	p-value
P53	Tumor Protein 53
p85	Regulatory Subunit of PI3K
PBS	Phosphate Buffered Saline
PCR	Polymerase Chain Reaction
PELP1	Proline-Glutamate and Leucine Rich Protein 1
PI3K	Phosphoinositide 3 kinase
PR	Progesterone Receptor
PVDF	Polyvinylidene Fluoride
RNA	Ribonucleic Acid
rpm	Rounds per minute
RPMI	Rose Park Memorial Institute
SDS	Sodium Dodecyl Sulfate
Sec	Second
SEM	Standard Error of the Mean
Src	Proto-oncogene Tyrosine-protein Kinase Src
TGF- β	Transforming Growth Factor Beta 1 Receptor
V	Volts
WNT	Wingless-type MMTV (mouse mammary tumor virus)
Mg	Micro Gram
ml	Micro Liter
μ M	Micro Molar

CHAPTER I

LITERATURE REVIEW

A. Mammary Gland

1. *Overview*

The mammary gland is located in the breasts of female mammals and functions in producing milk as nourishment for young offspring. It is a secretory organ consisting of multiple cell types including epithelial cells, which line the milk ducts and alveoli, and are made up of many luminal cells oriented toward the apex. In addition to the epithelial cells, the mammary gland is also composed of myoepithelial cells that contact the basement membrane and are basally oriented.

Furthermore, adipocytes form a large fraction of the stromal fat pad in addition to the presence of fibroblasts, immune, lymphatic and vascular cells (Inman et al., 2015).

2. *Development Processes & Pathways of the Mammary Gland*

The mammary gland development commences during embryonic life, stops at birth, and resumes at puberty (Watson & Khaled, 2008). Studies derived from mouse models represent the development of mammary glands in humans keeping into consideration the physical and genetic variability between both species (Lanigan et al., 2007).

On the tenth day of gestation, mammary lines are first observed between the fore and hind limb buds of the mouse embryo. Twenty-four to

thirty-six hours later, five pairs of lens-shaped mammary placodes form. Subsequent development and invagination of the placodes occur at embryonic day fourteen, thus mammary buds are formed. In humans, ductal branching is initiated around week sixteen and continues until puberty. Moreover, the ductal lumen and nipples develop at the same time. At puberty, mammary ducts, the ductal lumen and the nipples develop and continue doing so during pregnancy, the time of which the milk producing glands mature (Wysolmerski & Cowin, P., 2010).

The development of the mammary gland involves complex signaling especially at puberty. Ovarian and pituitary hormones, such as estrogen and growth hormones induce, through the release of various endocrine signals, the production of IGF1, HGF, EGF and FGF in a paracrine signaling manner. On the other hand, autocrine signaling is triggered by various cues such as transforming growth factor- β (TGF- β) that negatively controls mammary gland morphogenesis by inducing ECM production or by triggering non-canonical WNT signaling to inhibit proliferation and possibly regulate cell adhesion and migration (Nelso & Gjorevski, 2011).

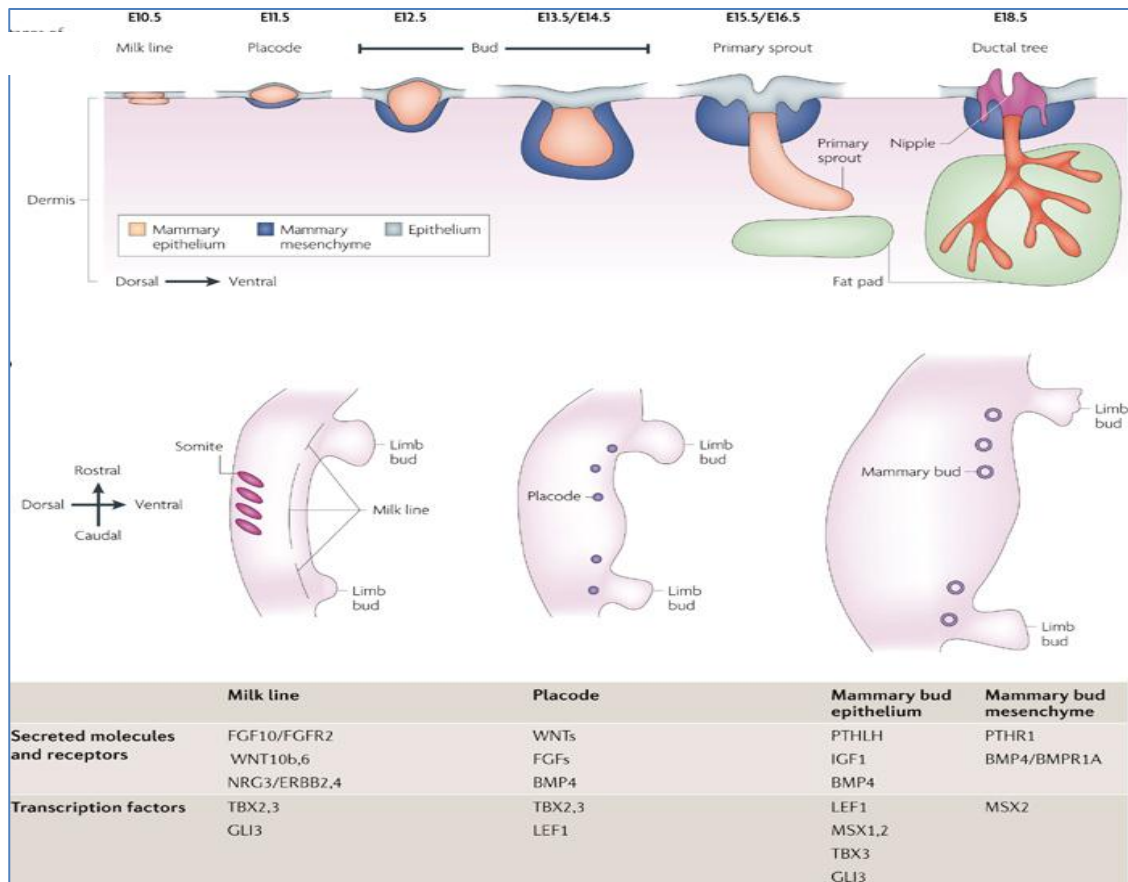


Figure 1: Stages of Development of the Mammary Glands (as modified from Robinson, 2007). The mammary lines first appear on the tenth day of gestation which transform into placodes, then buds. The buds are changed into primary sprouts that merge with fat pads to form the ductal tree on the eighteenth embryonic day. These stages are accompanied with the secretion of various signaling molecules and transcription factors.

B. Breast Cancer

1. Overview

Breast cancer is the most common type of cancer among women in the world and is the number one cause of cancer death in women despite improvements in diagnostic tools and treatments (Becker, 2015 & Bernard-

Marty et al., 2002). It can also occur in men; however, it is a hundred times less common in males than in females (Makki, 2015).

The main risk factor of breast cancer is age, and other risk factors include low parity and low rates of breast feeding (Becker, 2015) It can occur in any cell of the mammary gland cells, but breast carcinomas are the most common although various types of sarcomas and lymphomas can also be encountered (Makki, 2015).

Breast carcinomas can be ductal, occurring in the ducts, or lobular, in the lobules, and each can either be in situ or invasive. Ductal carcinoma in situ (DCIS) and lobular carcinoma in situ (LCIS) are noninvasive proliferations of epithelial cells in the ducts and lobules of the breast, respectively. On the other hand, invasive ductal carcinoma (IDC) and invasive lobular carcinoma (ILC) are malignant proliferations of neoplastic cells and penetrate into the stroma (Makki, 2015).

These breast carcinomas exhibit a wide range of morphological features, various immunohistochemical profiles and unique histopathological subtypes each having a specific clinical course and outcome (Makki, 2015).

2. *Breast Cancer Subtypes*

Clinicopathological variables such as tumor size, tumor grade and nodal involvement in addition to classical immunohistochemistry (IHC) markers are used to determine patient prognosis and management. IHC markers include estrogen and progesterone receptors, ER and PR

respectively, human epidermal growth factor receptor 2 (HER 2), the marker of proliferation Ki67 and basal markers (Dai et al., 2015).

Breast cancer is distinguished by four major molecular subtypes that vary according to the expression of IHC markers. Luminal A, which account for fifty percent of invasive breast cancers, overexpress ER and PR but not HER2 and are referred to as ER/PR positive and HER2 negative. This subtype is of low grade, grades 1 and 2, and usually of good prognosis. The other luminal subtype, luminal B, similar to luminal A is ER/PR positive. However, unlike luminal A, luminal B can be HER2 negative or positive with higher expression of proliferation index Ki67 than luminal A. Furthermore, luminal B cancers tend to be of higher grade and poorer prognosis than luminal A tumors. A third subtype is the HER2 overexpression which comprises fifteen percent of all invasive breast cancers. This subtype is ER/PR negative and, as its name implies, HER2 positive with high Ki67. Forty to Eighty percent of the HER2 overexpression tumors harbor TP53 mutations and are of high grade - usually grade 3 - and poor prognosis. The last major subtype is the basal-like one and is named so due to the fact that its pattern of expression is similar to basal epithelial cells and normal myoepithelial cells. It is referred to as triple negative because ER/PR and HER2 receptors are not over expressed. Nevertheless, it highly expresses the basal markers, cytokeratins 5/6, 14 and 17, with a high Ki67 index and commonly possess TP53 mutations. Basal-

like tumors represent fifteen percent of all invasive breast carcinomas and are of high grade and low survival rates (Makki, 2015).

Among the various cell lines established MCF-7 cells belong to the luminal A subtype and MDA-MB-231 cells belong to the basal subtype. These cells will be used in this study and represent a range of the different types of breast cancers.

C. Breast Cancer Treatment

1. Treatment Options

Mastectomy or surgical breast removal was introduced by Umberto Veronesi and Bernhard Fisher in the early 1970s and greatly improved the lives and fates of hundreds of thousands of women worldwide. Breast surgery, the basic treatment option, changed tremendously over the past years and attempts to reconstruct or conserve the breasts. Radiation oncology is a second treatment option for breast cancer and involves cancer cell eradication via high energy beams, and often accompanies surgical treatment. Systemic treatment consists of chemotherapeutic, hormonal, targeted and, more recently, immunotherapeutic drugs administered to patients (Becker, 2015).

2. Chemotherapy

Chemotherapy was first introduced in the 1950s to treat nonsolid tumors such as leukemia. Treatment for solid tumors was later presented during the 1970s with breast cancer being the model. Various regimens were developed during the past years beginning with cyclophosphamide,

methotrexate and 5-fluorouracil treatment leading to today's standard of epirubicin and cyclophosphamide followed by paclitaxel (Becker, 2015).

D. Paclitaxel

1. Overview

Paclitaxel, in addition to Docetaxel, is a commonly used cytotoxic drug for breast cancer. Both drugs possess favorable efficacy in metastatic breast cancer and early stage breast cancer. Besides breast cancer, Paclitaxel is used in the treatment of ovarian cancer, and non-small cell lung cancer (NSCLC) among others (Murray et al., 2012).

Paclitaxel was discovered in 1960 as part of the National Cancer Institute screening program in search for plant extracts with antineoplastic activity. Paclitaxel was isolated and identified by Drs. Wall and Wani in the bark of the Pacific Yew Tree or *Taxus brevifolia*. It was later introduced into clinical use in the 1990s (Murray et al., 2012 & Kingston, 2001).

2. Mechanism of Action of Paclitaxel

Paclitaxel mainly induces apoptosis by targeting tubulin. Paclitaxel binds to β -tubulin subunits of the microtubules enhancing their stable polymerization even in the absence of GTP. The number of protofilaments required for microtubule assembly is twelve in the presence of Paclitaxel instead of a normal average of thirteen. Moreover, Paclitaxel inhibits the catastrophe of microtubules or disassembly by calcium ions (Ca^{2+}) (Figure 1) (Barbuti & Chen, 2015). Subsequently, cells arrest at G₂/M phase and commit apoptosis. Additionally, Paclitaxel affects the cell cycle via

molecular mechanisms including the activation of cell division control-2 kinase (cdc-2) (Ibrado et al., 1998); stabilization of cyclin B-1 (Ling et al., 1998 & Yuan et al., 2006); activation of the spindle assembly checkpoint; phosphorylation of b-cell lymphoma 2 (bcl-2) (Berchem et al., 1999 & Wang et al., 1999) leading to apoptosis; and the inhibition of cell proliferation (Murray et al., 2012).

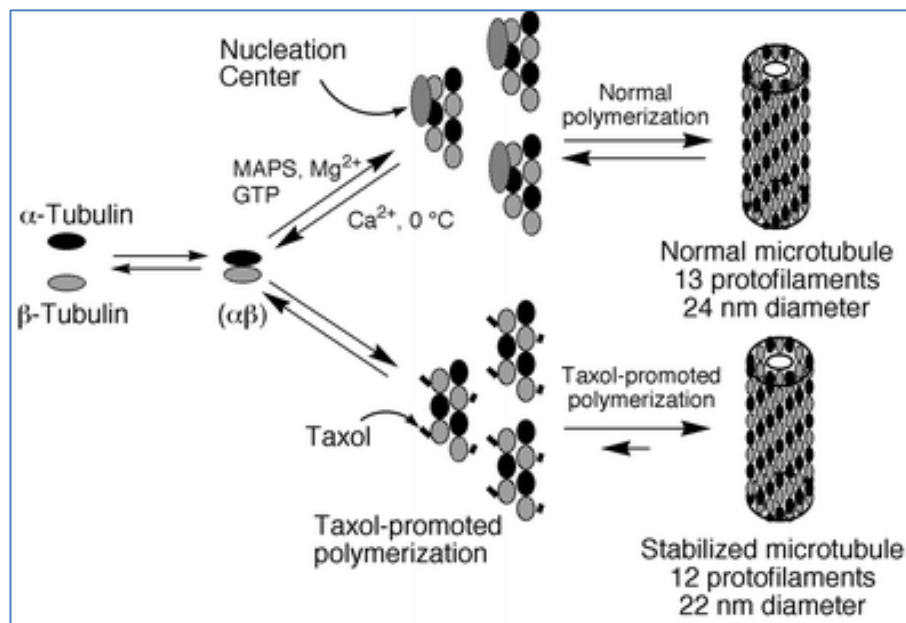


Figure 2: Mechanism of action of Paclitaxel (as modified from Kingston, 2001). Paclitaxel binds β -tubulin on the α/β proto-filaments inducing highly stable Paclitaxel-promoted polymers made up of 12 proto-filaments with a diameter of 22nm.

3. *Resistance Mechanisms of Paclitaxel*

a. Overview

One of the major limitations of chemotherapeutic drugs is the development of resistance. There are various cellular and molecular

mechanisms that contribute to chemoresistance in general. These mechanisms include modifications in membrane lipids, compartmentalization, induction of emergency response elements, changes in cell cycle checkpoint proteins, increase or alteration in drug targets, bio-inactivation, inhibited apoptotic responses, increased repair of DNA damage, decreased uptake, and increased efflux of the drug (Barbuti & Chen, 2015).

More specifically, Paclitaxel induces resistance through overexpression of ATP-binding cassette (ABC) transporters, reduced function of apoptosis proteins including Bcl-2 and p53, alterations in cytokine expression such as Interleukin-6, tubulin mutations, and alterations in binding regions of β -tubulin (Barbuti & Chen, 2015).

b. Tubulin Alterations Conferring Paclitaxel Resistance

Both α - and β -tubulin mutations modify the stability of microtubules without affecting the affinity of paclitaxel binding. These mutations are point mutations that could occur at various sites such as mutations at β 173 (proline to alanine) and β 292 (glutamine to glutamate) in class I β -tubulin, and a point mutation at residue 379 (serine to serine/ arginine) in K- α 1 tubulin (Barbuti & Chen, 2015 & Orr et al., 2003).

In addition to mutations in tubulin, β -tubulin isotype expression, specifically isotypes III and V, is altered in Paclitaxel resistant cells. Furthermore, Paclitaxel resistance may occur as a result of transformed

binding regions on the microtubules (Barbuti & Chen, 2015 & Orr et al., 2003).

Microtubules are regulated by microtubule associated proteins (MAPs) which include microtubule stabilizers, such as MAP4, and microtubule destabilizers like stathmin. Overexpression of microtubule destabilizers and/ or inactivation of microtubule stabilizers decrease the stability of microtubules and lead to Paclitaxel insensitivity (Barbuti & Chen, 2015 & Orr et al., 2003).

Modifications in microtubules may also result in response to post-translational modifications performed by various proteins (Barbuti & Chen, 2015 & Orr et al., 2003).

E. Tubulin Tyrosine Ligase-Like (TTL) Proteins

1. Overview

Post-translational modifications generally regulate the function of proteins and can be divided into mono-modifications and poly-modifications. Mono-modifications, which include phosphorylation and acetylation, add one molecule at the modification site. Poly-modifications, on the other hand, add side chains to the acceptor site and they consist of ubiquitinylation, polyglycylation and polyglutamylolation. These modifications, both the single molecule additions as well as the side chain additions, affect tubulin and microtubules. Polymodifications of microtubules result from the action of a family of tubulin tyrosine ligase-like (TTL) proteins (Van Dijk et al., 2007).

TLL proteins are a family of fourteen predicted proteins, thirteen of which were identified. These proteins are highly conserved among different species and share a core tubulin tyrosine ligase (TTL) domain, an extended TTL domain specific for each family member, and an ATP site (Van Dijk et al., 2007).

2. *Functions of TLL proteins*

TLL proteins are protein ligases that add a glycyl, acetyl or polyglutamyl side chains to microtubules. These post-translational modifications lead to the generation of microtubules with various lengths resulting in downstream signaling effectors. These changes also regulate the affinity between microtubules and MAPs, and are also important for centriole stability, axonemal motility and neurite growth. (Van Dijk et al., 2008).

TLL proteins can also target proteins other than tubulin. TLL proteins modify nucleosome assembly proteins 1 and 2, NAP1 and NAP2 respectively, thus altering the affinity of these proteins to their binding partners. (Van Dijk et al., 2008). Moreover, TLL proteins act on proline, glutamate and leucine-rich protein 1 (PELP1) (Kashiwaya et al., 2010), and retinitis pigmentosa GTPase regulator (RPGR) (Sun et al., 2015) among others. Interestingly, TLL4 was shown to polyglutamylate the chaperone, NAP, and the chromatin remodeler, PELP in red blood cells as well as

MAD2 leading to the maturation of megakaryocytes in the bone marrow and platelets in the peripheral blood (Ijaz et al., 2016).

3. *Polyglutamylation*

a. Overview

Polyglutamylation is a post-translational modification that involves the addition of glutamate amino acids on target proteins. (Van Dijk et al., 2008). It is a highly regulated reversible reaction. It is carried out by nine TTLs: TTL1, 2, 4, 5, 6, 7, 9, 11 and 13 (Wasylyk et al., 2010) and reversed by a family of proteins called carboxypeptidases (Ye et al., 2014).

b. Polyglutamylation on Tubulin

Polyglutamylation was initially identified on α -tubulins and β -tubulins which form the building blocks of microtubules. On α -tubulin, an initiation of polyglutamylation occurs where the first glutamate forms a covalent bond between its amino group and the γ -carboxyl group of the glutamate on the substrate protein. An elongation reaction follows resulting in subsequent glutamate addition (up to twenty in some cases). Similarly, polyglutamylation targets the C-terminal tail of β -tubulin. (Janke et al., 2008). As a result, polyglutamylation enhances cellular transport and modulates the interaction of the microtubules with their associated proteins including MAP tau, MAP1A, MAP1B and MAP2. (Garnham et al., 2015).

4. *Specific Activities of TTLLs*

All TTLLs mentioned above, except TTLL2, can act on tubulins, α and β (Wasylyk et al., 2010). Nevertheless, each TTLL is specific for α -tubulin and/or β -tubulin, and for the initiation and/or the elongation reaction. For example, TTLL4 is more specific to β -tubulin and solely initiates polyglutamylation. On the other hand, TTLL6 is more specific for α -tubulin and catalyzes the elongation reaction. (Van Dijk et al., 2007).

F. **Tubulin Tyrosine Ligase-Like Family Member 4 (TTLL4)**

1. *Overview*

Tubulin Tyrosine Ligase-Like family member 4 is a 133 kDa protein that is able to add a polyglutamyl group to its substrate proteins. TTLL4 along with the family member 7 (TTLL7) are highly specific to β -tubulin which is the site preferred by Paclitaxel. Both TTLL4 and TTLL7 are highly specific to the initiation reaction of polyglutamylation; however, TTLL4 is not involved in the elongation reaction while TTLL7 is which makes TTLL4 more specific to the initiation reaction of polyglutamylation. In addition, TTLL4 is also highly specific to NAP proteins, unlike TTLL7, which may suggest signaling interaction with the nucleus. (Janke et al., 2008). Furthermore, TTLL4 was shown to be overexpressed in many types of cancer and immunotherapy targeting this protein was recently patented by Nakamura *et al.* as a method of treatment and prophylaxis. (Nakamura et al., 2013).

2. The Different Isoforms of TLL4 & Protein Modification

TLL4 has ten protein coding isoforms in addition to two nonsense isoforms. The coding isoforms include transcripts and proteins of various base pairs and molecular weights, respectively. There are two transcripts one made up of 4967 bp and of 4730 bp that code for 1199 aa proteins with 133.38 kDa Molecular weights. The other transcripts are made up of 3971 bp, 3723 bp, 747 bp, 738 bp, 712 bp 601 bp, 588 bp and 583 bp that code for the 125.66 kDa, 109.5 kDa, 18.89 kDa, 27.22 kDa, 10.61 kDa, 18.99 kDa, 10.53 kDa and 23.01 kDa respectively (Aken et al., 2016).

Table 1: The Various TLL4 Isoforms					
Trascript Name	bp	Protein	Biotype	Molecular Weight (g/mol)	Molecular Weight (kDa)
TLL4-001	4967	1199aa	Protein coding	133,378.36	133.38
TLL4-201	4730	1199aa	Protein coding	133,378.36	133.38
TLL4-003	3971	1135aa	Protein coding	125,657.38	125.66
TLL4-002	3723	973aa	Protein coding	109,401.46	109.40
TLL4-007	747	174aa	Protein coding	18,890.60	18.89
TLL4-015	738	246aa	Protein coding	27,221.01	27.22
TLL4-006	712	101aa	Protein coding	10,613.09	10.61
TLL4-016	601	162aa	Protein coding	18,990.56	18.99
TLL4-008	588	100aa	Protein coding	10,526.01	10.53
TLL4-020	583	194aa	Protein coding	23,012.78	23.01
TLL4-018	811	179aa	Nonsense mediated decay	No protein	
TLL4-019	476	100aa	Nonsense mediated decay	No protein	

Table 1: The Different Isoforms of TLL4 (Aken et al., 2016).

Moreover, TLL4 undergoes various post-translational modifications itself. These modifications include various phosphorylation sites in addition to some sites that undergo acetylation and ubiquitylation.

Furthermore, these modifications are not only present in human TTLL4 but also in rat and mouse TTLL4 proteins with some alterations in the modification sites] (“Cell Signaling Technology”, 2017).

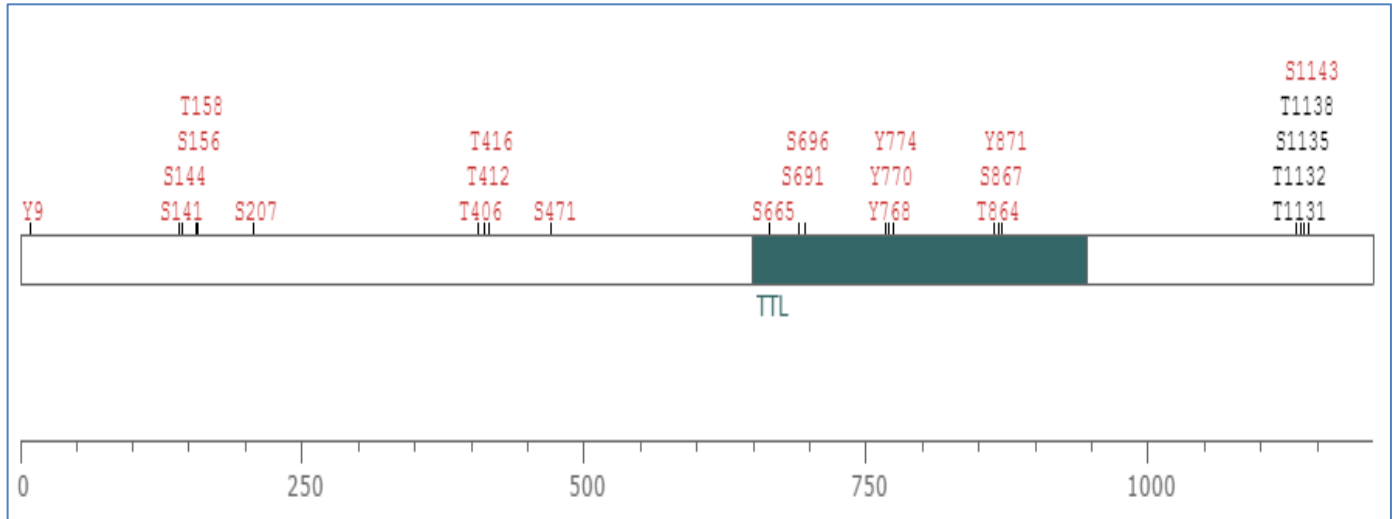


Figure 3: Phosphorylation Sites on humanTTLL4 (1199 a.a.) [modified] (“Cell Signaling Technology”, 2017).

3. *Role of TTLL4 in Cancer*

TTLL4 seems to be overexpressed in many types of cancers including bladder cancer, chronic myelogenous leukemia (CML), liver cancer, rectal cancer, prostate cancer, pancreatic cancer, osteosarcoma, small lung cancer and non-small lung cancer. (Nakamura et al., 2013). Nevertheless, TTLL4 is well studied in pancreatic cancer where its exogenous induction causes increased growth of the cancer cells as opposed to decreased growth in case TTLL4 is knocked down. TTLL4 was proved to interact with PELP1 and activate it by polyglutamylation which in turn plays

a role in activating Src, ER, p85 of PI3K and is involved in H3 acetylation.

(Kashiwaya et al., 2010).

G. Gap in Knowledge, Study Rationale and Hypothesis

TLL4 associates with the cytoskeleton and allows for initiating the polyglutamylation of tubulin leading to elongation and branching of the microtubules (Janke, 2014). Therefore, TLL4 may have a role in modulating cytoskeletal stiffness, and henceforth invasion and several other hallmarks of tumor cells. However, the expression of TLL4 and its putative role in breast cancer have not been adequately researched yet.

Moreover, it has long been reported that Paclitaxel has no effect on α -tubulin polyglutamylation, but stimulates that of β -tubulin in young differentiating mouse brain neurons (Audebert et al., 1993) which can be explained by Paclitaxel's specific binding to the β -subunit of tubulin (Orr et al., 2003 & Rao et al., 1992). Furthermore, among many factors that could contribute to Paclitaxel resistance in cancer cells such as mutations, and tubulin isotype selection, it has been proposed that post-translational modifications to tubulin and changes in the levels of proteins that regulate microtubule dynamics by lieu of their interaction with the tubulin dimers or the polymerized microtubules have the potential to alter the sensitivity of cells to Paclitaxel. These post-translational modifications include polyglutamylation and polyglycylation of both tubulin subunits (Rao et al., 1992). More recently, Septin was shown to cooperate with tubulin polyglutamylation to contribute to adaptation of cancer cells to taxanes (Froidevaux-Klipfel et al., 2015).

We hereby hypothesize that TTLL4 expression and/ subcellular localization is altered in breast cancer and that its expression levels influence cellular sensitivity to Paclitaxel. It is also plausible that TTLL4 expression, subcellular localization &/or enzymatic activity are modulated in response to treatment with Paclitaxel.

H. Objective of the Study and Specific Aims

The objective of the study is to evaluate the expression of TTLL4 at the transcript and protein levels in breast cancer cell lines with Paclitaxel and under baseline conditions. The proposed study is comprised of three main specific aims subdivided:

Specific Aim 1 – Quantify TTLL4 transcript levels in MCF7 and MDA-MB-231 breast cancer cell lines under standard conditions and after treatment with suboptimal and IC₅₀ doses of Paclitaxel. Specific tasks include:

MDA-MB-231 and MCF-7 cells were treated with suboptimal and optimal doses of Paclitaxel and RNA was extracted after 0.5, 2 and 8 hours of treatment. The obtained RNA was reverse transcribed to cDNA which in turn underwent Real-time PCR assessing the transcript levels of TTLL4.

Specific Aim 2 - Measure TTLL4 protein levels in MCF7 and MDA-MB-231 breast cancer cell lines under standard conditions and upon treatment with suboptimal and IC₅₀ doses of Paclitaxel by IF, Western Blot & ELISA. Specific tasks include:

MDA-MB-231 and MCF-7 cells were treated with suboptimal and optimal doses of Paclitaxel and the cells were fixed after 6, 12 and 24 hours of treatment. The cells were probed for TTLL4 according to the immunofluorescence procedure optimized for and subsequently visualized under fluorescence microscope. MCF-7 cells were treated with suboptimal and optimal doses of Paclitaxel and protein was extracted after 6, 12 and 24 hours of treatment followed by Western blot.

Specific Aim 3 - Assess TTLL4 subcellular localization in MCF7 and MDA-MB-231 breast cancer cell lines under standard conditions and upon treatment with suboptimal and IC₅₀ doses of Paclitaxel by IF. Specific tasks include:

MDA-MB-231 and MCF-7 cells were treated with suboptimal and optimal doses of Paclitaxel and the cells were fixed after 6, 12 and 24 hours of treatment. The cells were probed for TTLL4 according to the immunofluorescence procedure optimized for and subsequently visualized under fluorescence microscope.

I. Significance of the Study

Investigating the overexpression of TTLL4 in breast cancer cell lines will provide new insights into the role the protein plays in breast cancer and cancer in general. Determining that TTLL4 is overexpressed in breast cancer upon Paclitaxel treatment allows for better personalized and targeted therapies for breast cancer patients. Furthermore, new information about TTLL4 and its essentiality would reveal new targets for breast cancer therapy including immunotherapy.

CHAPTER II

MATERIALS AND METHODS

A. Maintenance of Cells in Tissue Culture

1. MCF-7

MCF-7 is a human breast adenocarcinoma cell line derived from a pleural effusion. The cell line was kindly provided by Dr. Rabih Talhouk's laboratory, Department of Biology, AUB. The cells were cultured in RPMI 1640 media (Sigma-Ibra Haddad) to which 1% Pen-Strep and 10% Fetal Bovine Serum (Sigma-Aldrich) are added. The doubling time for the cells is about 29hrs. When the cells reach an 80% density confluence, they are washed with 1× Phosphate Buffered Saline (PBS) (Lonza) then detached with 2×Trypsin (Lonza) after 3mins of incubation at 37°C, 5% CO₂ incubator. Complete media is then added to neutralize the trypsin and the cells are centrifuged at 600g and 4°C for 5min. Subsequently, the cell pellet is suspended in 1ml of complete media and distributed in 10cm plates pre-filled with 10ml growth media.

2. MDA-MB-231

MDA-MB-231 is a human breast adenocarcinoma cell line with a highly invasive phenotype. It was also provided by Dr. Rabih Talhouk's laboratory. The culture media and protocol for maintaining this cell line are similar to the one used for MCF-7 cells, but the trypsinization time is about 30secs. The doubling time for the cells is about 26hr.

3. Cell Count

Trypan blue vital exclusion stain and a hemocytometer were used to accurately determine the number of viable cells from the total population of cells in a 10cm plate. Post-resuspension of the cell pellet in 1ml of complete growth medium, a sample of the cells was removed and diluted 1:10 for counting. An appropriate volume of cells (depending on seeding density) was then removed and mixed with the required volume of complete media in order to be distributed to cell culture plates.

B. RNA Extraction

RNA samples were isolated from MCF-7 and MDA-MB-231 cells under the following conditions:

1. Baseline Conditions

MCF-7 and MDA-MB-231 cells were seeded in 6 well plates at a density of 6×10^4 cells/ml in complete RPMI media. At 80% confluence, the cells were rinsed once with PBS(1X) and RNA was extracted from the corresponding panel of breast cancer cells using the TRI Reagent (TRIzol, Cat.# T9424, Sigma-Aldrich) according to the manufacturer's specifications. RNA samples were quantified and assessed for purity and integrity using the Nanodrop Spectrophotometer (Thermonanodrop 2000C, Central Research Science Lab (CRSL) facility, AUB) then stored at -70°C .

2. Paclitaxel Treatment

MCF-7 cells were seeded in 12 well plates with seeding density being 6×10^4 cells/ml in complete RPMI media. When the cells reached 80% confluence, they were treated with two suboptimal doses of Paclitaxel (Cat # T7402, Sigma-Aldrich) 14nmol/L and 55nmol/L,

and the IC₅₀ dose 220nmol/L (Motiwala & Rangari, 2015) in addition to 0nM control for 8hrs, 2hrs and 30mins. The doses were tested using trypan blue exclusion assays.

For every repeat, Paclitaxel was freshly prepared by serially diluting a sample of the stock with concentration 5.86mmol/L into 586µmol/L then 58.6µmol/L. This intermediate dilution was further diluted to one working stock with a concentration of 0.586µmol/l and another working stock of concentration 0.0586µmol/l. Final Paclitaxel concentrations of 220nmol/l and 55nmol/l were prepared from the first working stock, and the 14nmol/l concentration was prepared from the second. A final volume of 2ml from each dilution replaces the media in each of the four wells at the specific time points (8hrs, 2hrs and 30 mins). Post treatment, the cells were rinsed once with PBS (1X) and RNA extraction from MCF-7 cells was performed using TRI Reagent (TRIZol, Cat.# T9424, Sigma-Aldrich) according to the manufacturer's specifications. A vehicle of 0.1% DMSO was added to one of the wells at each time point and used as a control. RNA samples were then stored at -70°C. The samples were later quantified and assessed for purity and integrity using the Nanodrop Spectrophotometer (Thermonanodrop 2000C, Central Research Science Lab (CRSL) facility, AUB).

MDA-MB-231 cells were seeded in 12 well plates with seeding density being 6×10^4 cells/ml in complete RPMI media. At 80% confluence, the cells were treated with two suboptimal doses of Paclitaxel (Cat # T7402, Sigma-Aldrich) 20nmol/L and 80nmol/L, and the IC₅₀ dose 320nmol/L (Constantini *et al.*, 2016) in addition to 0nM control for 8hrs, 2hrs and 30mins. The doses were tested using trypan blue exclusion assays. A treatment protocol was done similar to MCF-7 cells.

3. Verification via RNeasy

In order to verify the lack of contamination by DNA using the TRIzol RNA extraction, RNA was extracted from MDA-MB-231 cells at baseline conditions by means of RNeasy® Plus MiniPrep Kit (Cat. # 74134, QIAGEN). The cells were split and cultured in 10cc plates at 5% CO₂ in complete RPMI 1640 media until they reached 80% confluence. Once the desired confluence is reached, MDA-MB-231 cells were lysed using 600 µl of Buffer RLT and vortexed for 30sec. The lysate is transferred to a gDNA Eliminator spin column placed in the provided 2 ml collection tube. The sample is then centrifuged for 30sec at 8000g. The column containing the DNA is discarded and 600 µl of 70% ethanol is added to the eluent. A volume of the sample, 700 µl, is transferred to the RNeasy spin column placed in a supplied collection tube. The sample is then centrifuged for 15sec at 8000g, and the resulting flow-through is discarded. Subsequently, 700 µl of Buffer RW1 is added to the RNeasy column placed in collection tube and centrifuged for another 15sec at 8000g. After that, 500µl of Buffer RPE is added to the spin column which is centrifuged for 15sec at 28000g. The flow-through is discarded and the same volume of Buffer RPE is added, but the sample is centrifuged for 2mins at 8000g. To elute the RNA, the RNeasy spin column is placed in a new collection tube and 50µl of RNase-free water is added to the column which is centrifuged for 1min at 8000g.

C. Reverse Transcription

cDNA reverse transcription was performed on the extracted RNA from each sample using the iScript cDNA Synthesis Kit (Bio-Rad) following the manufacturer's protocol specifications. Briefly, 1µg of RNA was mixed with 1µl of the reverse transcriptase

enzyme, 4µl of the Reaction Mix, and 16µl of nuclease free sterile water in a total volume of 20µl. The reverse transcription protocol consists of 3 steps: 5mins at 2°C, 30mins at 42°C, then followed by 5mins at 85°C. The samples were stored at -20°C (Malkhassian L MSc Thesis, 2012).

D. Real-Time PCR

Real-Time PCR amplification was performed using the iQ SYBR Green Supermix (Bio-Rad) and specific primer pairs for each selected gene. The primer sequences for the Real-Time PCR amplification of the selected genes were computationally derived from the MGH/Harvard Medical School Primer Bank Database (Table 1). The reverse transcribed cDNA was diluted to a 1:10 ratio (10µl cDNA with 90µl nuclease free sterile water). Then 2.5µl of nuclease free sterile water, 1µl of the reverse primer for each gene, 1µl of the forward primer for each gene and 12.5µl mastermix were added to 8µl of the diluted cDNA derived from the different samples in a total volume of 25µl. The reaction was achieved using a Real-Time PCR machine (Bio-Rad) with the following protocol: a heating step for DNA denaturation starting with 50°C which was then increased to 95°C for 10mins. Subsequently, the temperature was lowered to 60°C for 1min to allow the primers to anneal to their complementary strands after which the temperature was shifted to 72°C for 30secs. This cycle was repeated 44 times. The final step was completed at the same temperature but for 10mins. All experimental results were analyzed by the BIO-Rad CFX Manager Software.

Table 2: A list of the forward and reverse primers used to quantify genes by Real-Time PCR.		
Gene	Primer	Sequence 5'-3'
<i>GAPDH</i>	Forward	AAGGTGAAGGTCGGAGTCAAC
	Reverse	GGGGTCATTGATGGCAACAATA
<i>TLL4</i>	Forward	TCTCTCCCGGACTTGTTCAAC
	Reverse	TGCTGGTACGGTTTTTGCCTA

E. Protein Extraction, SDS-PAGE & Western Blot Analysis

1. Protein Extraction

a. Baseline conditions

MCF-7, MDA-MB-231 and wild type MEF cells were grown in 10 cc culture dishes and left to reach 80% confluence in 10ml of complete media, at 37°C and 5% CO₂. The cells were washed twice with 3ml pre-cooled PBS (1X) per culture plate. Cells in each plate were then lysed using 300µl of standard RIPA lysis (R0278, Sigma-Aldrich) buffer in addition to fresh Protease Inhibitor Cocktail (Cat# P-8340, Sigma-Aldrich) at 1:1000. Samples were then incubated in the cold room 30min. After wards, lysate clusters were lodged off the plates using a micropipette tip. Cell lysates were then centrifuged at 12000xg at 4°C for 10mins. Following centrifugation, supernatants containing protein extracts from different samples were transferred to new pre-labeled, sterile and precooled microfuge tubes.

b. Paclitaxel Treatment

MCF-7 cells were seeded in 6 well plates at 10×10^4 cells/ml in complete media. When the cells reached 80% confluence, they were treated with 14, 55 and 220 μ M of Paclitaxel for 24h, 12h and 6h. Post Paclitaxel treatment, the cells were rinsed twice with pre-cooled PBS (1X) using 0.5ml /well. Cells were then lysed using 100 μ l/well of standard RIPA lysis buffer supplemented with Protease Inhibitor Cocktail (Cat# P-8340, Sigma-Aldrich) at 1:1000 freshly added at the time of use. Samples were then incubated in the cold room 30min. After wards, lysate clusters were lodged off the 6 well plates using a micropipette tip. Cell lysates were then centrifuged at 12000xg at 4°C for 10mins. Following centrifugation, supernatants containing protein extracts from different samples were transferred to new pre-labeled, sterile and precooled microfuge tubes. Samples were then stored at -20°C.

2. Sample Protein Quantification

To quantify the proteins, a standard of specific dilutions of 1mg/ml of Bovine Serum Albumin (BSA) (Cat.# 0332, Amresco) in deionized distilled water (ddH₂O) was prepared in the first two lanes of a 96 well plate. The standards were prepared in duplicates with the following BSA content (μ g): 0.0, 2.0, 4.0, 6.0, 8.0, and 10.0. 5 μ l of each sample was placed in duplicate in the subsequent lanes. After wards, 200 μ l of the Optiblot Bradford Reagent (Cat.# ab119216, Abcam) was added to each well and measurement of protein contents was performed using the SpectraMax ascent software (Multiskan EX, Thermo lab Systems).

3. SDS-PAGE: Sodium Dodecyl Sulfate-Polyacrylamide Gel Electrophoresis

a. Casting & Running the Gel

Whole cell lysates from MCF-7 cells cultured Post- Paclitaxel treatment were resolved by a 12% Tris-HCl buffer providing an optimal separation of the small- to medium- sized proteins. The resolving and the stacking gels were hand casted using short plates and spacer plates with 1.5mm integrated spacers. The short plate and spacer plate were evenly aligned and slid into the casting frame. The casting frame was then placed into the casting stand while ensuring its proper alignment to prevent leakage. To prepare 1.5mm thick resolving or lower gel, 4.8ml of 30% Acrylamide/Bis (Cat.# 161-0158, Bio-Rad) were mixed with 3ml of 1.5M Tris-HCl pH 8.8 (Cat.# 161-0798, Bio-Rad) and 4.2ml of deionized distilled water. 210 μ l of APS (Ammonium Persulfate, Cat.# 161-0700, Bio-Rad) and 30 μ l of TEMED (Tetramethylethylenediamine, Cat.# 0761, Ultra-pure grade, 59 Amresco) were then added to the resolving gel solution. The mixture was smoothly poured to the lower green mark of the casting frame using a glass or a disposable plastic pipette after which was immediately overlaid the top of the resolving gel with isobutanol to prevent it from drying and allow it to cast smoothly. The resolving gel was left for 45mins to polymerize. Similarly, a 1.5mm thick stacking or upper gel was prepared by mixing 750 μ l of 30% Acrylamide/Bis with 1.25ml of 0.5M Tris-HCl pH 6.8 (Cat.# 161-0799, Bio-Rad) and 3ml of deionized distilled water. 140 μ l of APS and 20 μ l of TEMED were then mixed with the stacking gel solution and poured between the glass plates until the top of the short plate was reached. The comb was seated between the glass plates by securely aligning the comb ridge with the top of the short plate, and the stacking gel was left to polymerize and

solidify for 15mins. Meanwhile, 1X MOPS running buffer was prepared by measuring 14.4g of glycine (Cat.# 161-0724, Bio-Rad), 2.5g of Tris-base (Cat.# 161-0719, Bio-Rad) and 1g of SDS (Sodium Dodecyl Sulfate, Cat.# 161-0302, Bio-Rad). The mixture was dissolved in 1L of deionized distilled water on a stirrer at room temperature. Casted gels were placed into the clamping frame in the electrophoresis cell or running chamber with the short plate facing inward while sliding both arms of the clamping chamber over the gels, locking them into place. Subsequently, the chamber was filled with 1X running buffer, the combs were removed slowly and the formed wells were rinsed thoroughly with the running buffer.

b. Preparing & Loading the Samples

40µg of total protein per sample was prepared by adding to each pre-cooled sterile microfuge tube the appropriate volume of the protein sample, deionized distilled water and 5X sample buffer (composed of glycerol, SDS, 0.5M Tris-HCl pH 6.8 and 60 traces of bromophenol blue). A previously prepared 5X sample buffer stored at -20°C was freshly mixed with 10% β-mercaptoethanol prior to each use. Samples were then denatured at 95°C for 5mins using a Thermobloc machine and placed directly on ice to prevent protein refolding. Later, the samples were loaded slowly using gel loading tips allowing them to evenly settle on the bottom of the wells. Precision Plus Protein standard (Cat.# 161- 0373, Bio-Rad) used as a molecular weight marker for the determination of the protein size was also loaded (5µl). The electrophoretic cell was covered with a lid in an orientation that matches the color coded plugs on the electrode assembly and electrical leads were inserted into the power supply. SDS-PAGE was then run at 200V for 45min until the tracking dye in

the sample buffer reached the bottom of the gel. Ice-buckets surrounded the running chamber shortly after the beginning of the run to prevent overheating.

c. Protein Transfer from Gel to Blot

Subsequent to the molecular weight-based migration of proteins through the gel, proteins were transferred from the gel onto a polyvinylidene fluoride (PVDF) transfer membrane (Immuno-Blot™ PVDF Membrane, Cat.# 162-0177, Bio-Rad). The PVDF membrane was cut to the desired size of the gel using a blotting paper as a reference. The membrane was activated by soaking it in 100% methanol (Sigma-Aldrich) for 1min under the fume hood. It was then incubated in ice cold transfer buffer (1X). The standard buffer for wet transfer is the same as the (1X) Tris-glycine buffer used for the running buffer; however, instead of adding SDS, methanol was added to a final concentration of 20%. The buffer was left to completely dissolve in an Erlenmeyer flask on a stirrer and was later stored at 4°C. Sponges 61 (two/gel) and thin blotting papers (two/gel) cut to the same size of the gel were also soaked in the transfer buffer. The running buffer was poured-off the running chamber and the gel was released from the clamping frame. Meanwhile, a gel releaser was used to remove the gel and submerge it in the transfer buffer. The gel and membrane sandwich was tightly assembled by placing the membrane and the gel between the buffer-soaked blotting papers in this order: white cassette→ sponge→ blotting paper→ PVDF membrane→ gel→ blotting paper→ sponge→ black cassette ensuring that no air bubbles were trapped between the membrane and the gel. Then, the assembled gel and membrane sandwich was placed in the transfer unit with the black side of the unit facing the black cassette and the red side facing the white cassette of the sandwich. Transfer buffer (1X) was then poured into the

transfer cell and a cooling unit was added. The transfer cell was then placed in a Styrofoam box covered in ice. We connected the transfer cell to the power supply and started the run at 100V for 2hrs. Later, the blotting papers and the gel were discarded in polyacrylamide waste containers.

d. Membrane Blocking, Washing & Antibody Incubations

Each membrane was incubated in 50ml of 5% BSA prepared in 0.1% PBS-T to block the non-specific sites on the membrane. Incubation was performed at room temperature on the ProBlot™ Rocker 25 at 60 rpm for 1hr. The blocking solution was prepared by weighing 2.5g of BSA and adding it to 25ml of 0.1% PBS-T. The solution was vortexed for few minutes until the BSA was completely dissolved in the washing buffer. The washing buffer (0.1% PBS-T) was prepared by adding to 100ml of 10X non-sterile PBS without Ca and Mg, 900ml of deionized distilled water and adjusted to a pH of 7.2. 1ml of Tween20 (Polyoxyethylene sorbitol ester, Cat.# P1379, Sigma-Aldrich) was then added to the 1L of PBS-T (1X) at a final concentration of 0.1%. Each membrane was incubated in a plastic pouch with 25 ml of the blocking solution prepared. After blocking, each membrane was incubated with goat anti-TTLL4 (S-14) (goat polyclonal IgG, 200µg/ml, used at 1:1000, Santa Cruz Inc.; Cat. # sc-169734) primary antibody diluted in 3-5ml of 5% BSA prepared in 0.1% PBS-T at 4°C on a ProBlot™ Rocker 25 at 60 rpm overnight. GAPDH primary antibody was employed as a loading control for normalization within each experiment. The next day, each membrane was placed in a plastic case and washed three times in 20ml of the 0.1% PBS-T washing buffer at room temperature on a ProBlot™ Rocker 25 at 90 rpm, 10mins each. The membranes were incubated in plastic

pouches with a Horseradish peroxidase (HRP)-conjugated Donkey anti-goat secondary antibody used at 1:2500 and obtained from Abcam (Cat# ab97110) on a ProBlot™ Rocker 25 at 60 rpm for 1hr at room temperature. Post incubation with the secondary antibody, each membrane was washed in 20ml of 0.1% PBS-T washing buffer at room temperature for three times 10min each on a ProBlot™ Rocker 25 at 90 rpm.

e. X-ray Film Imaging of Western Blots

Western Lightening Chemiluminescence Reagent (ECL Western Blotting Substrate Kit, Abcam) composed of Reagent A (ab65628) and Reagent B (ab65629) were used to develop the signal using autoradiography X-ray film (AGFA) and XOMAT X-ray film processor (Optimax). In brief, 1ml of each reagent was added to the probed membrane placed in a plastic case in the dark. The membrane was left for 1min for the chemical reaction to occur while gently agitating the plastic case. Afterwards, the membrane was transferred to a cassette (Spectroline Monotec Cassette, Spectronics Corp.) and covered with a plastic pouch. The chemiluminescent signal was detected and recorded by exposure of the membrane to a light-sensitive autoradiography X-ray film inserted into the cassette in the dark room. The films were exposed for 30sec, 1min and 2mins when the membrane was probed for TTLL4 (S-14). In addition, films were exposed for 1min when probing for GAPDH primary antibody.

f. Membrane Stripping & Re-probing with a Different Primary Antibody

Membrane-bound antibody-protein complex were stripped using 10ml of 0.1M NaOH (Sodium hydroxide) prepared by diluting 1M NaOH in deionized distilled water at

room temperature for 45min. Post stripping, each membrane was washed for few minutes with 10ml of 0.1% PBS-T washing buffer. Subsequently, each membrane was blocked in 5% BSA prepared in 0.1% PBS-T as mentioned earlier at room temperature on a ProBlot™ Rocker 25 at 60 rpm for 1hr. This was followed by incubation with 3-5ml of primary antibody such as GAPDH prepared in 5% BSA in 0.1% PBS-T washing buffer on a ProBlot™ Rocker 25 at 60 rpm for 1hr. The membrane is washed three times as previously mentioned with 0.1% PBST washing buffer for 10min each and incubated with the HRP-conjugated secondary antibody directed against the species of the primary antibody. Western Blot experiment was completed thereafter by washing the membrane with 0.1% PBS-T for three times 10min each and developing a chemiluminescent signal using an autoradiography X-ray film (AGFA) as stated previously.

F. Immunofluorescence Staining

1. Baseline Conditions

MCF-7 and MDA-MB-231 cells were seeded at 6×10^4 cells/ml in 6- well plates on 22 x 22 mm wide and 0.17-0.25 mm thick square cover glass (Corning) using 4ml of complete media per well. Cells were allowed to adhere to reach 80 % confluence at 37°C, 5% CO₂. Cells were then washed twice with PBS (2mL/well) for 5min each time in a biosafety cabinet. After wards, under the fume hood, the cells were fixed with 200µL of pre-cooled (-20⁰C) methanol per slide and left for 10mins in the fridge at -20°C. The excess methanol was removed under the fume hood and the cells permeabilized with pre-cooled acetone and left at -20°C for 1min. Later, the cells were washed three times with PBS

(2mL/well); 5min per wash. A blocking solution of 2% BSA in PBS (2mL per well) was added for 1 hour then removed to wash the cells once with PBS (2mL/well) for 5 minutes. After blocking, the cells were incubated with the goat anti-TTLL4 (goat polyclonal IgG, 200µg/ml, used at 1:50, Santa Cruz Inc.; Cat. # sc-169734) primary antibody diluted in 1% BSA in PBS (300 µL/ slide) for 1 hour. Following primary antibody incubation, the cells were re-washed three times with PBS (2mL/well) for 5 minutes each. After which, the cells were incubated with fluorescent Alexa 488-conjugated secondary antibody (donkey antigoat IgG-HRP; Abcam; Cat. # ab97110) diluted 1:100 in PBS (200 µL/ slide) for 1 hour. The DNA in the nuclei were counterstained with one drop of the UltraCruz™ Hard-set Mounting Medium provided as a 10ml solution containing 1.5µg/ml of 4',6-diamidino-2-phenylindole (DAPI) onto the glass slides. The coverslips were placed cell side down in a forward motion after removing excess of 1X PBS remaining on the coverslip due to the washing steps by simply holding the coverslip vertically against a kim wipe. Excess mounting medium flowing out from under the coverslips and spilling on the sides were removed using the tip of a folded kim wipe. This was followed by sealing the edges of the coverslips with nail polish and placing the slides in a slide box in the dark at 4⁰C for 48h before microscopic imaging.

2. Paclitaxel Treatment

MCF-7 cells were seeded at 6×10^4 cells/ml in 6- well plates on 22 x 22 mm wide and 0.17-0.25 mm thick square cover glass (Corning) using 4ml of complete media per well. Cells were allowed to adhere to reach 80 % confluence at 37°C, 5% CO₂. When the cells reached 80% confluence, they were treated with 14, 55 and 220µM of Paclitaxel for

24h, 12h and 6h. Post Paclitaxel treatment, the samples were processed as mentioned previously.

G. Microscopic Imaging

TTLL4 intensity was visualized using the fluorescence microscope (Leica) in the Central Research Science Laboratory, AUB and the Confocal Microscope in the Faculty of Medicine, AUB. Cells stained with the secondary antibody only were used as negative controls for the experiment.

H. Enzyme Linked Immunosorbent Assay (ELISA)

Various sample extraction methods were utilized to assess TTLL4 expression using ELISA. MCF-7 cells were treated with 0nM and 14nM Paclitaxel for 24hrs at 37°C, 5% CO₂.

Complete RPMI 1640 media was aspirated and cells were extracted using RNeasy supplied RLT Buffer. The cells were vortexed for 30s and the lysates transferred to a gDNA eliminator spin columns placed in 2ml collection tubes. The cells were centrifuged for 30s at 8,000g after which the columns were discarded and 600µl of 70% ethanol were added to the flow-through. Then, 700µl of the samples were transferred to RNeasy spin columns and centrifuged for 15s at 8,000g. The protein in the flow-through is precipitated by centrifuging for 10mins at 13,300g and dissolved in 500µl of PBS(1X) with 1:1000 protease inhibitor cocktail.

In another method, media was aspirated and the cells were trypsinized and centrifuged for 5mins at 4⁰C and 600g. The cells were then washed with 1X PBS and centrifuged with the same parameters. After this, two lysis buffers were used to lyse the cells. The first is made up of 150mM Histidine (pH=7.4), 100µl of Triton X100 and 1:1000 protease inhibitor cocktail. The second consists of 50mM KCl, 1.5mM MgCl₂, 10mM Hepes Buffer and 1:1000 protease inhibitor cocktail. After lysis, cells were homogenized and assessed by ELISA.

Sonication was attempted after media aspiration and cell washing. The cells were dissolved in a solution of 50mM Tris-HCl (pH=7.5) and 1:1000 protease inhibitor cocktail. The cells were shocked with ultrasound waves in a water bath sonicator (filled with ice and water) at 100% intensity for 3 shocks for 15s each and 25s ice incubation between each stimulus.

50µl of the obtained samples were placed in Human Tubulin Polyglutamylase TTLL4 ELISA wells (Cat. # MBS9334568, MyBioSource) in addition to 50µl of each standard (20, 10, 5, 2.5, 1.25 and 0.625ng/ml) and 50µl of the sample diluent (the blank provided). Then, 100µl of HRP-conjugate reaction was added to each well and left to be incubated at 37⁰C for 60 mins. After the incubation, the wells were washed 4 times with 1X wash buffer supplied, and 50µl of each of Chromogen Solutions A and B were added to the wells and incubated 37⁰C for 15 mins. Then 50µl of stop solution was added to each well and the optical density was measured at 450nm using the ELISA spectrophotometer machine.

I. Statistical Analysis

The statistical analyses were done using one way ANOVA and independent samples t-test. The calculations were achieved using SPSS program. A p-value of 0.05 represents the statistical significance. Furthermore, the average of each group, the standard deviation and the standard error of the mean were calculated and a comparison of each group to their control group was done. Unless mentioned otherwise, all experiments were performed in duplicates three independent times.

CHAPTER III

RESULTS

A. Optimization of Paclitaxel Treatments

The IC₅₀ doses of Paclitaxel for MCF-7 and MDA-MB-231 cells were published to be 220nM and 320nM respectively. Initially, those cells were attempted to be treated by immunofluorescence and western blot for 24hrs, 2hrs and 30 mins. Living MCF-7 (Figure 4A and B) and MDA-MB-231 (Figure 4 C and D) cells were counted by trypan blue cells exclusion. However, after looking into the molecular weight of the protein, approximately 6hrs is needed by the cells to produce the first batch of TTLL4 enzyme, and at 24hrs, the protein production is almost saturated with 12hrs being the intermediate between both. At the transcript level, 30mins is the required time to produce the first RNA batch of TTLL4, 8hrs is the time of saturation, and 2hrs the intermediate time.

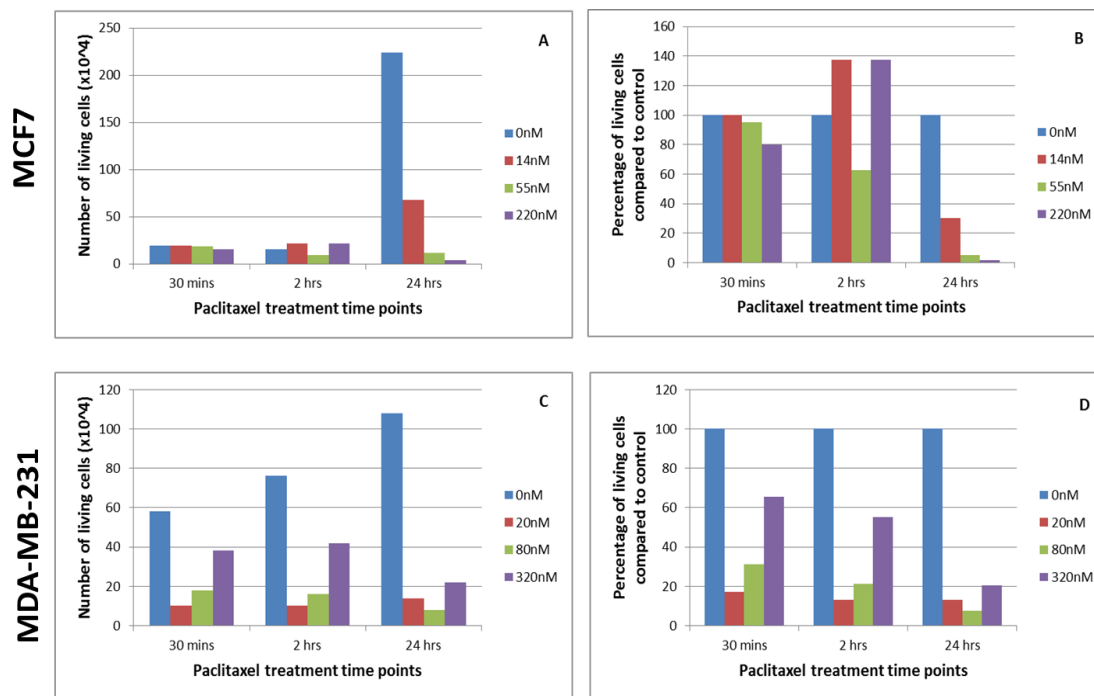


Figure 4: Counts of MCF-7 and MDA-MB-231 cells for Paclitaxel treatment optimization. Panels A&C: Number of living cells in MCF-7 and MDA-MB-231 cells respectively at the different Paclitaxel concentrations and the various time points. Panel B&D: Percentage of living cells with respect to the control in MCF-7 and MDA-MB-231 cells respectively at the different Paclitaxel concentrations and the various time points.

B. Assess expression of *TLL4* transcriptional levels under baseline conditions and upon treatment with Paclitaxel in MCF-7 and MDA-MB-231 cell lines.

1. *MCF-7* cells significantly express more transcript levels of *TLL4* under baseline conditions in comparison to *MDA-MB-231* cells.

One part of the first aim was to determine transcriptional expression levels of *TLL4* in MCF-7 and MDA-MB-231 cells under baseline conditions. As such, quantitative Real-Time PCR (qRT-PCR) experiments were performed on both types of cells post RNA extraction and reverse transcription while securing consistency in cell density, spreading as well as confluency across the samples and throughout independent repeats. Under baseline conditions and after normalization to the transcriptional levels of

GAPDH reference gene, Real-Time PCR quantification data revealed that the expression of *TLL4* in MCF-7 cells was 3-fold \pm 0.15 higher than transcript *TLL4* expression in MDA-MB-231 cells. This expression was statistically significant with a p-value <0.05 . The data represent mean fold difference \pm SEM of three independent repeats, each done in duplicates.

(Figure 5, see below).

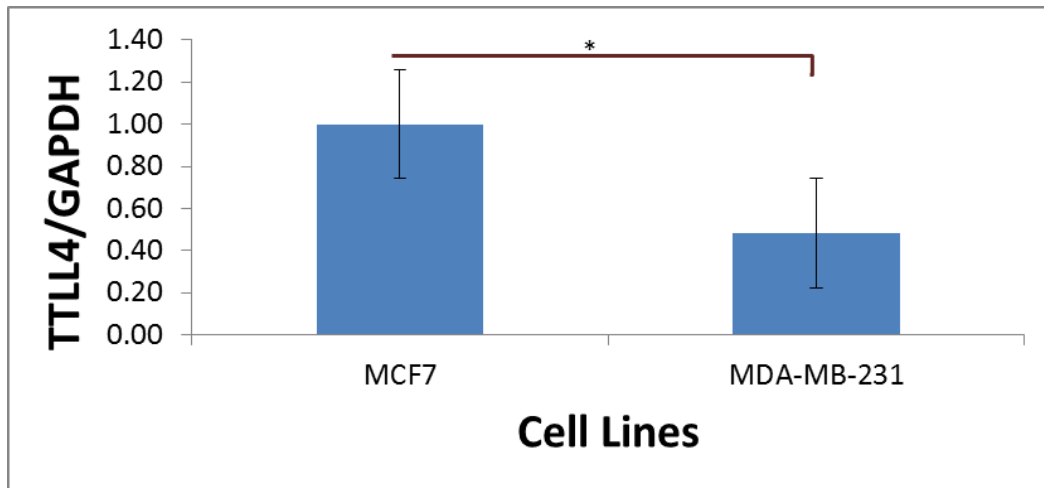


Figure 5: Mean fold change in *TLL4* transcript expression in MCF-7 and MDA-MB-231 cells at baseline conditions. Real-Time PCR quantification data suggest that the *TLL4* transcript expression is higher in the MCF-7 cell line than in the MDA-MB-232 cell line. *TLL4* transcript expression was normalized to that of the *GAPDH* reference gene. Data represent mean fold difference \pm SEM in comparison derived from 3 independent experiments; each performed in duplicates. One asterisk represents a statistical significance ($P < 0.05$) by t-test.

2. No significant change in *TLL4* expression in MCF-7 cells upon Paclitaxel treatment.

Another part of the aim was to assess transcript *TLL4* levels in MCF-7 cells upon treatment with Paclitaxel. MCF-7 cells were treated with Paclitaxel concentrations of 0nM, 18nM, 55nM and 220nM for 30 mins, 2

hrs and 8 hrs. Afterwards, quantitative Real-Time PCR (qRT-PCR) experiments were executed upon RNA extraction and reverse transcription while ensuring consistency in cell density, spreading as well as confluency across the samples and throughout the independent repeats. Upon Paclitaxel treatment and after normalization to the transcriptional levels of *GAPDH* reference gene, Real-Time PCR quantification data illustrated that the expression of *TLL4* in MCF-7 cells was not significantly amplified. However, *TLL4* transcript levels were elevated with 14nM Paclitaxel at 8 hrs, 55nM Paclitaxel at 30 mins and 2 hrs, as well as with 220nM Paclitaxel at the three timepoints in comparison with the control of 0nM Paclitaxel concentration. The data represent mean fold difference \pm SEM of four independent repeats, each done in duplicates. (Figure 6, see below).

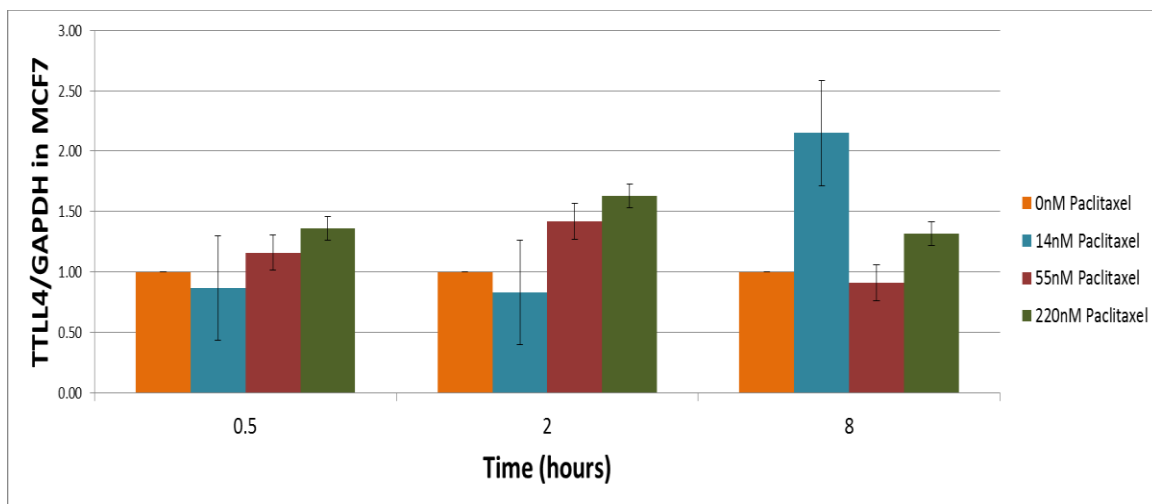


Figure 6: Mean fold change in *TLL4* transcript expression in MCF-7 post-Paclitaxel treatment. Real-Time PCR quantification data suggest that the *TLL4* transcript expression in the MCF-7 cell line is not significantly altered upon treatment with Paclitaxel. *TLL4* transcript expression was normalized to that of the *GAPDH* reference gene. Data represent mean fold difference \pm SEM in comparison derived from 4 independent experiments; each performed in duplicates.

3. No significant change in *TLL4* expression in MDA-MB-231 cells upon Paclitaxel treatment.

Following the second part of the first aim was evaluating transcript *TLL4* levels in MDA-MB-231 cells upon treatment with Paclitaxel. MDA-MB-231 cells were treated with Paclitaxel concentrations of 0nM, 20nM, 80nM and 320nM for the same time points of 30 mins, 2 hrs and 8 hrs. Quantitative Real-Time PCR (qRT-PCR) experiments were completed once RNA extraction and reverse transcription were performed with consistent cell density, spreading as well as confluency across samples and over the independent repeats. After Paclitaxel treatment and normalization to the transcriptional levels of *GAPDH* reference gene, Real-Time PCR quantification data illustrated that the expression of *TLL4* in MDA-MB-231 cells was not significantly augmented. However, *TLL4* transcript levels were modulated with 20nM Paclitaxel at 30 mins, 80nM and 320nM Paclitaxel at the three time points in comparison with the control of 0nM Paclitaxel concentration. The data represent mean fold difference \pm SEM of four independent repeats, each done in duplicates. (Figure 7, see below).

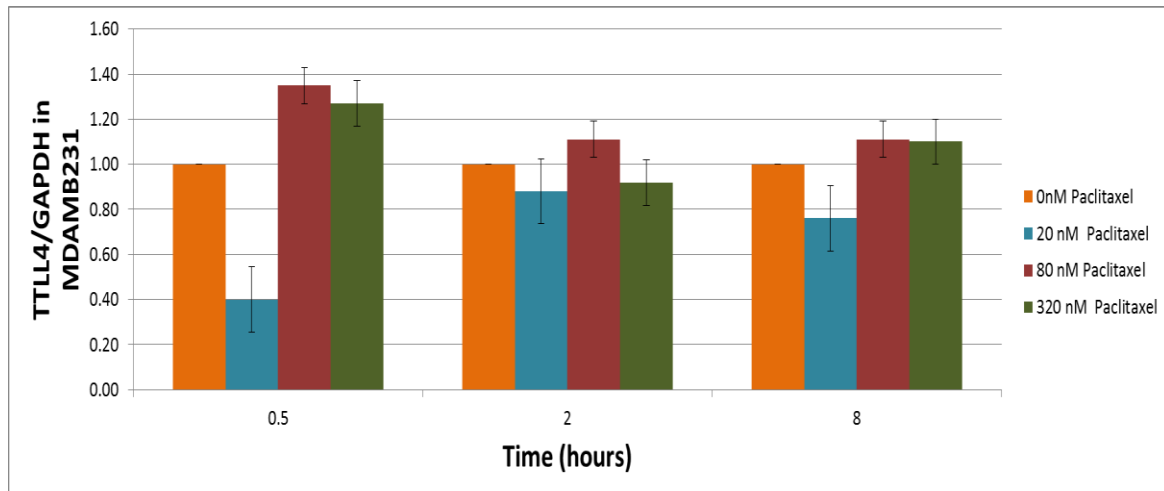


Figure 7: Mean fold change in *TLL4* transcript expression in MDA-MB-231 cells post-Paclitaxel treatment. Real-Time PCR quantification data suggest that the *TLL4* transcript expression in the MDA-MB-231 cell line is not significantly altered upon treatment with Paclitaxel. *TLL4* transcript expression was normalized to that of the *GAPDH* reference gene. Data represent mean fold difference \pm SEM in comparison derived from 4 independent experiments; each performed in duplicates.

4. No significant change in *TLL4* and *GAPDH* Cq values in MDA-MB-231 cells between TRIzol and RNeasy RNA extraction.

There was some uncertainty regarding the purity of the extracted RNA with TRIzol. Therefore in order to assess that the RNA extraction was void of contamination, *TLL4* and *GAPDH* Cq values were determined upon TRIzol and RNeasy extraction from MDA-MB-231 cells under baseline conditions. Afterwards, quantitative Real-Time PCR (qRT-PCR) experiments were executed upon the RNA extracts and reverse transcription was performed while ensuring consistency in cell density, spreading as well as confluency across the samples and throughout the independent repeats. After normalization to the transcriptional levels of *GAPDH* reference gene, Real-Time PCR quantification data illustrated that the Cq values of *TLL4* in MDA-MB-231 cells was not significantly altered. The data represent

mean fold difference \pm SEM of two independent repeats, each done in duplicates. (Figure 8, see below).

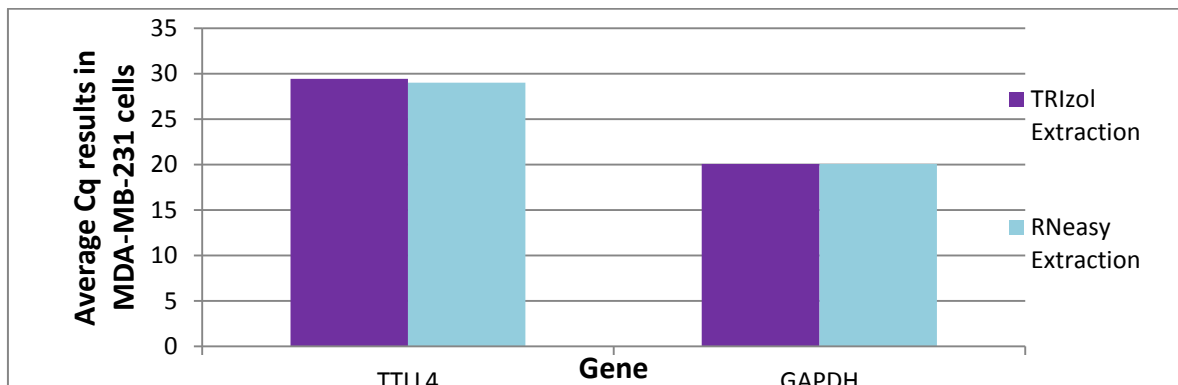


Figure 8: Mean fold change in *TLL4* transcript expression in MDA-MB-231 under baseline conditions by TRIzol versus RNeasy RNA extraction. Real-Time PCR quantification data suggest that the *TLL4* Cq values in the MDA-MB-231 cell line are almost identical. *TLL4* transcript expression was normalized to that of the *GAPDH* reference gene. Data represent mean fold difference \pm SEM in comparison derived from 2 independent experiments; each performed in duplicates.

C. Investigate potential changes in TLL4 protein expression levels under baseline conditions and upon treatment with Paclitaxel in MCF-7 and MDA-MB-231 cell lines.

1. *TLL4* protein is differentially expressed in MCF-7 and MDA-MB-231 cell lines under baseline conditions by immunofluorescence staining.

To examine possible alterations in the TLL4 protein distribution and localization in MCF-7 and MDA-MB-231 cells under baseline conditions, immunofluorescence staining was performed on methanol fixed cells with TLL4 antibody. Using identical exposure time, six image frames were obtained per slide for each of the above mentioned cell lines. The data suggest a higher protein expression in MCF-7 cells than in MDA-MB-231

cells (Figure 9A). Images of each of the cell lines were also taken in 3D (Figure 9B).

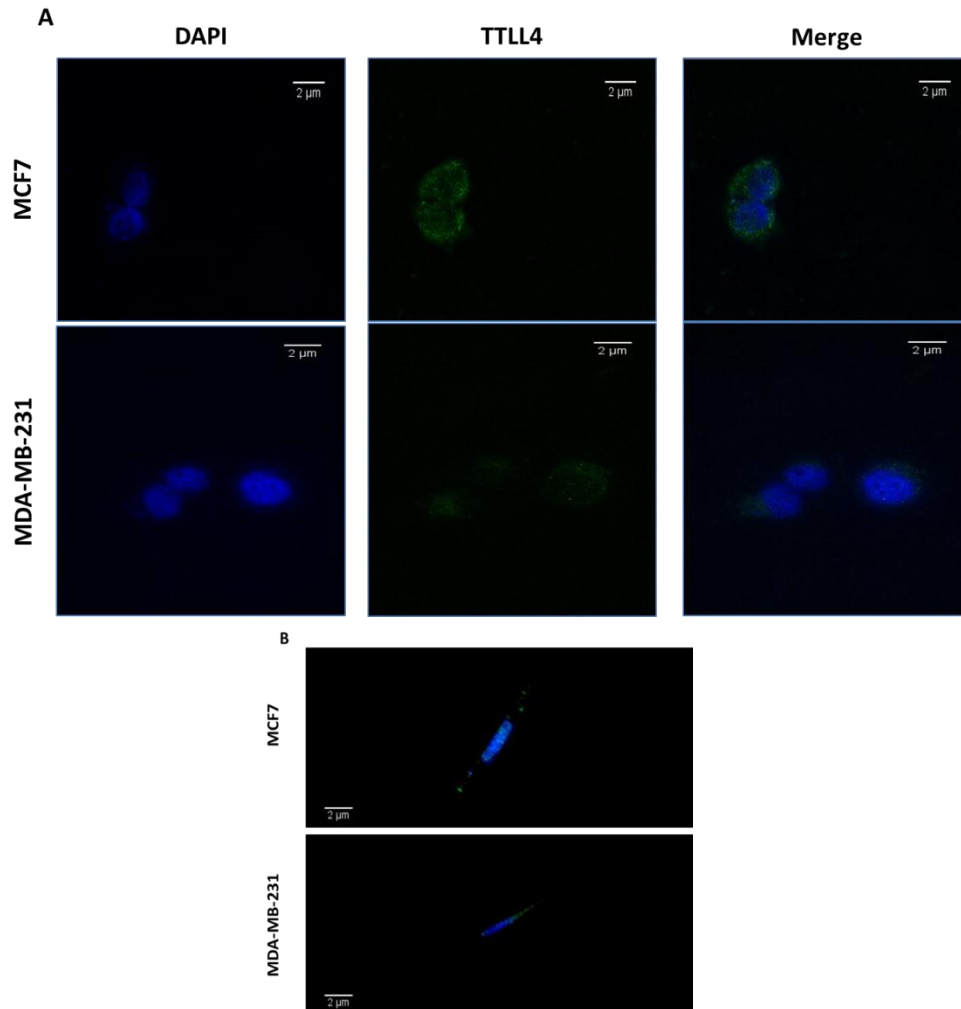


Figure 9: Immunofluorescence staining of TTLL4 protein in MCF-7 and MDA-MB-231 cells under baseline conditions. Panel A: representative upright fluorescence microscope images showing immunofluorescence staining of TTLL4 in MCF-7 and MDA-MB-231 cells. DAPI was used to stain the nuclei. Images were acquired at 40X magnification. Panel B: representative 3D confocal microscope images showing immunofluorescence staining of TTLL4 in MCF-7 and MDA-MB-231 cells. DAPI was used to stain the nuclei. Images were acquired at 60X magnification.

2. *TTLL4* protein is distinctly expressed in MCF-7 cell line post-Paclitaxel treatment by immunofluorescence staining.

To study possible alterations in the TTLL4 protein distribution and localization in MCF-7 upon Paclitaxel treatment, immunofluorescence staining was performed on methanol fixed cells with TTLL4 antibody. Using identical exposure time, six image frames were obtained per slide for the MCF-7 cells at the different concentrations (0nM, 14nM, 55nM and 220nM) and different time points (6hrs, 12hrs and 24hrs represented in Figures 10A, B and C respectively). The data suggest a higher protein expression in MCF-7 cells at the higher Paclitaxel concentrations (55nM and 220nM). Furthermore, the increase in TTLL4 upon Paclitaxel treatment also increases with time. Images of each of the cell lines were also taken in 3D. The scale bar refers to 20 μ m.

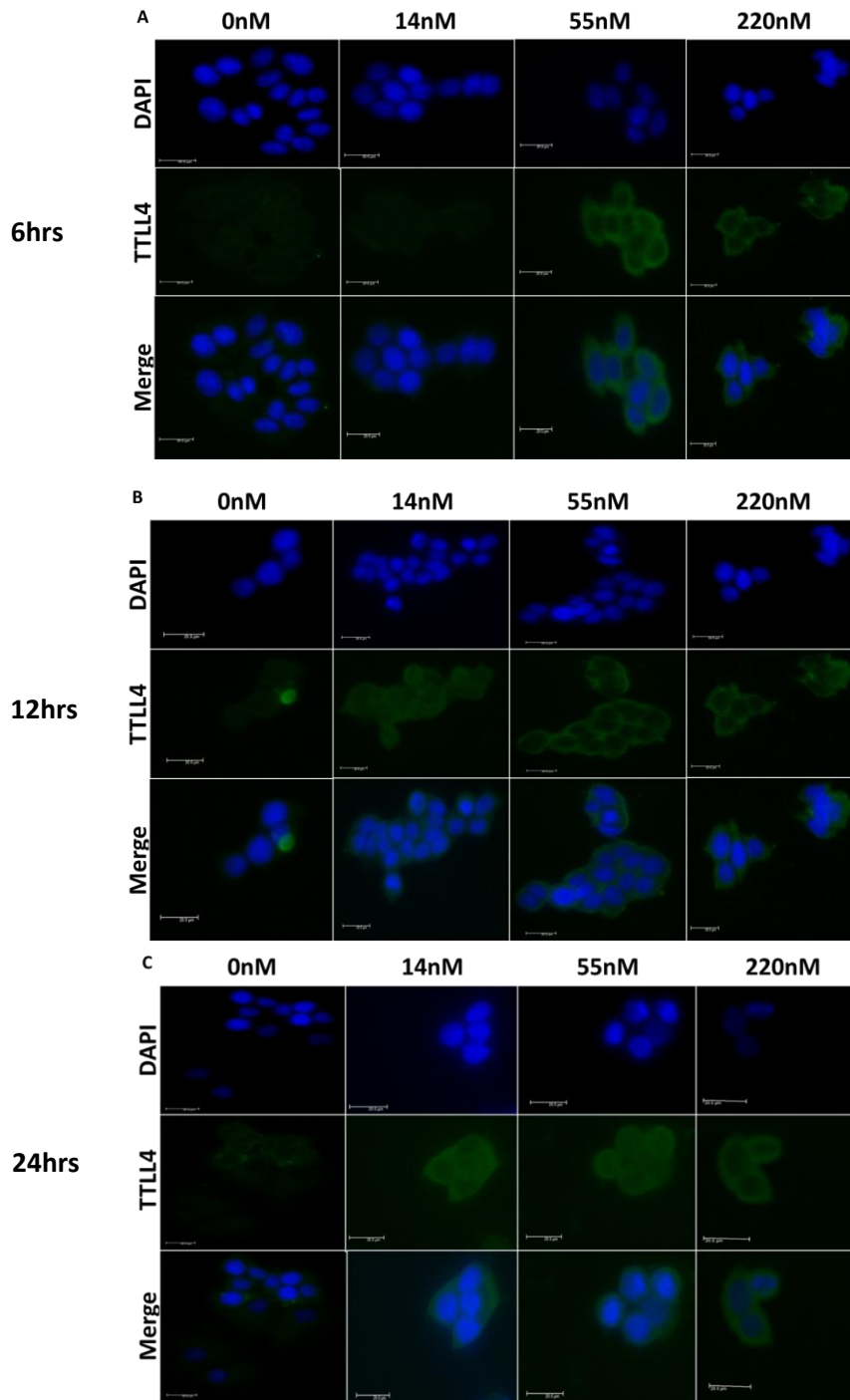


Figure 10: Immunofluorescence staining of TLL4 protein in MCF-7 cells after Paclitaxel treatment (0nM, 14nM, 22nM and 220nM). Panel A: representative upright fluorescence microscope images showing immunofluorescence staining of TLL4 in MCF-7 after 6hrs of treatment. DAPI was used to stain the nuclei. Images were acquired at 40X magnification. Panel B: representative upright fluorescence microscope images showing immunofluorescence staining of TLL4 in MCF-7 after 12hrs of treatment. DAPI was used to stain the nuclei. Images were acquired at 40X magnification. Panel C: representative upright fluorescence microscope images showing immunofluorescence staining of TLL4 in MCF-7 after 24hrs of treatment. DAPI was used to stain the nuclei. Images were acquired at 40X magnification.

3. TTLL4 protein is distinctly expressed in MDA-MB-231 cell line post-Paclitaxel treatment by immunofluorescence staining.

To study possible alterations in the TTLL4 protein distribution and localization in MDA-MB-231 upon Paclitaxel treatment, immunofluorescence staining was performed on methanol fixed cells with TTLL4 antibody. Using identical exposure time, six image frames were obtained per slide for the MDA-MB-231 cells at the different concentrations (0nM, 20nM, 80nM and 320nM) and different time points (6hrs, 12hrs and 24hrs represented in Figures 11A, B and C respectively). The data suggest a higher protein expression in MDA-MB-231 cells at the higher Paclitaxel concentrations (80nM and 320nM). Furthermore, the increase in TTLL4 upon Paclitaxel treatment also increases with time. Images of each of the cell lines were also taken in 3D. The scale bar refers to 20 μ m.

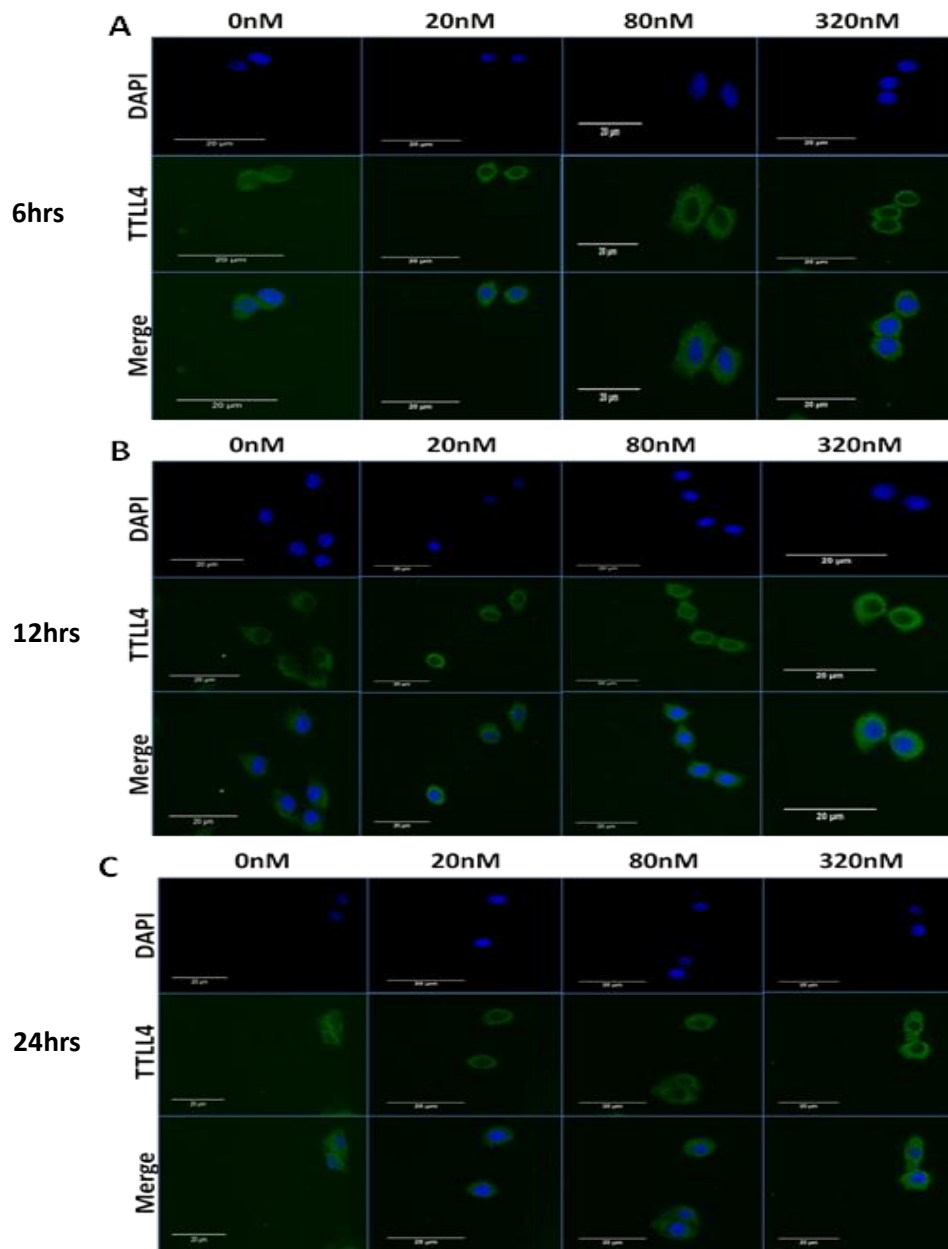


Figure 11: Immunofluorescence staining of TLL4 protein in MDA-MB-231 cells after Paclitaxel treatment (0nM, 20nM, 80nM and 320nM). Panel A: representative upright fluorescence microscope images showing immunofluorescence staining of TLL4 in MDA-MB-231 after 6hrs of treatment. DAPI was used to stain the nuclei. Images were acquired at 40X magnification. Panel B: representative upright fluorescence microscope images showing immunofluorescence staining of TLL4 in MDA-MB-231 after 12hrs of treatment. DAPI was used to stain the nuclei. Images were acquired at 40X magnification. Panel C: representative upright fluorescence microscope images showing immunofluorescence staining of TLL4 in MDA-MB-231 after 24hrs of treatment. DAPI was used to stain the nuclei. Images were acquired at 40X magnification.

4. *TTLL4* protein in MCF-7 and MDA-MB-231 cell lines under baseline conditions by Western Blot.

To determine any alteration at the protein level in TTLL4 expression under baseline conditions, MCF-7 and MDA-MB-231 cells were seeded to reach 80% confluence. Subsequently, protein extraction from total cell lysates, SDS-PAGE, and Western Blot analysis were performed using human anti-TTLL4 antibody from Santa Cruz and Abcam companies (Figure 12A and B, respectively). GAPDH was used a loading control for each (Figure 12C and D). Qualitative assessment was achieved by the visual detection and comparison of densitometry signals developed on autoradiography films. Under baseline conditions, MCF-7 and MDA-MB-231 cells express various TTLL4 isoforms including those possessing post-translational modifications. However, it was difficult to discern the difference in TTLL4 expression between the cell lines.

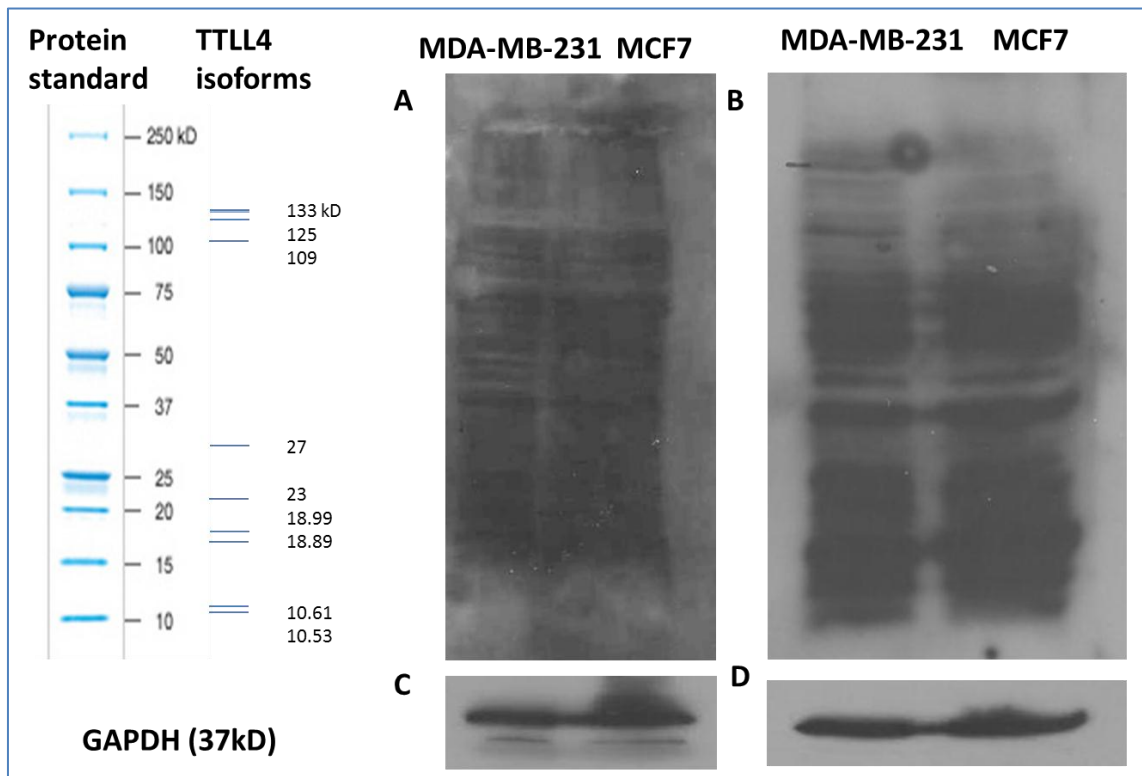


Figure 12: Western Blot of TLL4 protein expression in MCF-7 and MDA-MB-231 cells under baseline conditions. Panel A: representative blot of TLL4 expression in MCF-7 and MDA-MB-231 cells using the goat anti-TLL4 antibody from Santa Cruz. Panel B: representative blot of TLL4 expression in MCF-7 and MDA-MB-231 cells using the rabbit anti-TLL4 antibody from Abcam. Panels C&D: representative blots of the loading control GAPDH (37kDa).

5. *TLL4* protein in MCF-7 cells post-Paclitaxel treatment by Western Blot.

To determine any alteration at the protein level in TLL4 expression post-Paclitaxel treatment, MCF-7 were seeded and treated with 0nM, 14nM, 55nM, and 220nM Paclitaxel concentration for 6hrs, 12hrs and 24hrs. Then, proteins are extracted from total cell lysates, SDS-PAGE, and Western Blot analysis were performed using human anti-TLL4 antibody from Santa Cruz (Figure 13A) with GAPDH used as a loading control for (Figure 13B). Qualitative assessment was achieved by the visual detection and comparison of densitometry signals developed on autoradiography films. Upon

Paclitaxel treatment, MCF-7 cells express TTLL4, but it is difficult to distinguish the difference in TTLL4 expression between the different concentrations and time points. Nevertheless, the blots indicate an increased TTLL4 expression upon treatment with 220nM Paclitaxel at 6hrs, 55nM at 12hrs and 24hrs, and 14nM at 24hrs which goes in line with the immunofluorescence data. The most expressed isoform in the MCF-7 cell line is of molecular weight 27kDa; furthermore, a faint band of the 23 kDa isoform is also visible.

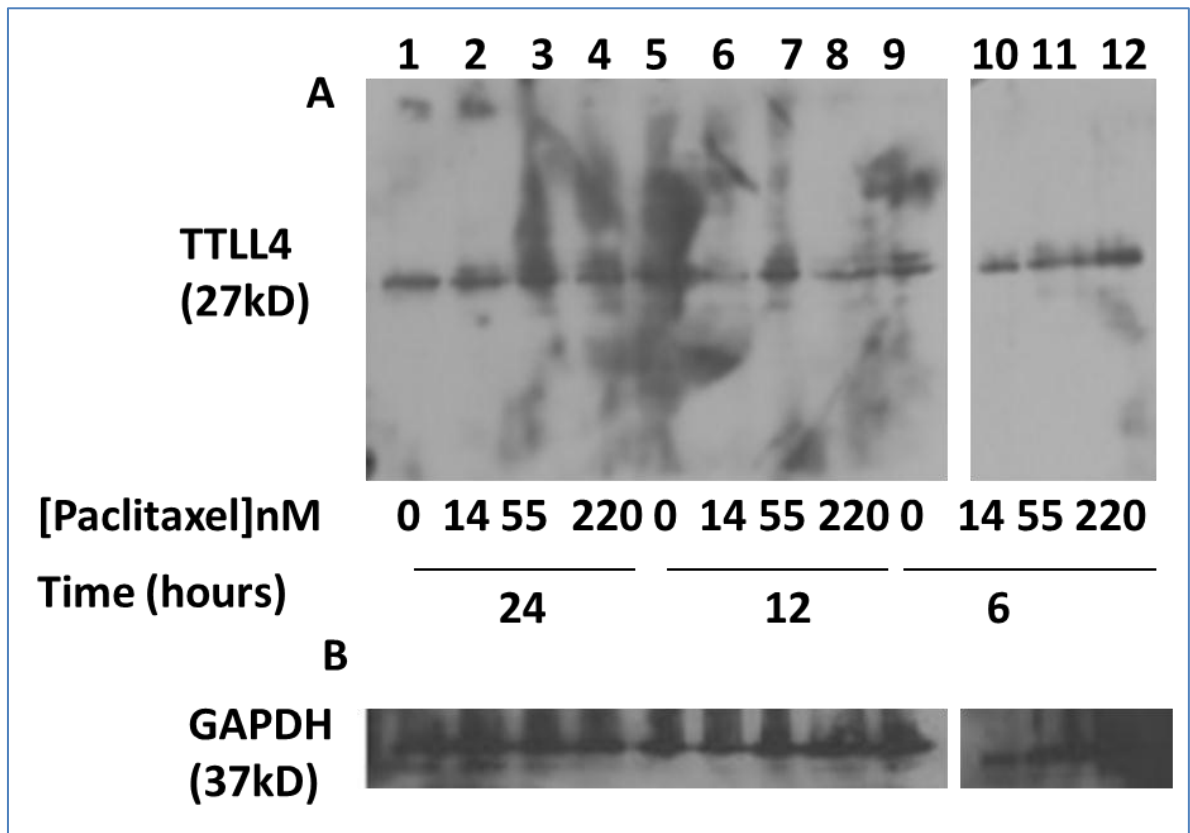


Figure 13: Western Blot of TTLL4 protein expression in MCF-7 after treatment with Paclitaxel. Panel A: representative blot of TTLL4 expression in MCF-7 cells using the goat anti-TTLL4 antibody from Santa Cruz. Panel B: representative blot of the loading control GAPDH (37kDa).

6. *TTLL4* protein in wild type MEFs under baseline conditions by Western Blot.

In order to determine whether the expression of the various TTLL4 isoforms are restricted to the breast cancer cell lines or this pattern of expression is visualized in other cell lines, the protein expression was examined in the wild-type MEF cell line. Protein extraction from total cell lysates, SDS-PAGE, and Western Blot analysis was executed in our lab using human anti-TTLL4 antibody from Santa Cruz and Abcam companies of two protein concentrations (20 and 30 μ g in the first and second wells respectively) (Figure 14A and B, respectively). GAPDH was used a loading control for each (Figure 14C). Qualitative assessment was achieved by the visual detection and comparison of densitometry signals developed on autoradiography films. Under baseline conditions, wild-type MEFs express various TTLL4 isoforms as well. However, each antibody detects a certain set isoforms of the enzyme.

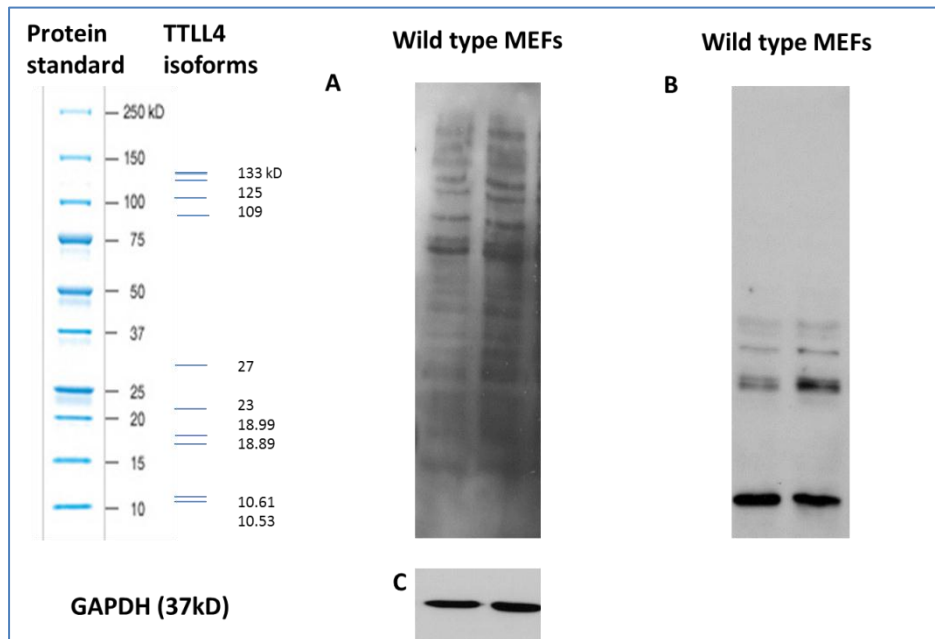


Figure 14: Western Blot of TLL4 protein expression in wild-type MEFs under baseline conditions. Panel A: representative blot of TLL4 expression in wild-type MEFs using the goat anti-TLL4 antibody from Santa Cruz. Panel B: representative blot of TLL4 expression in wild-type MEFs using the rabbit anti-TLL4 antibody from Abcam. Panel C: representative blot of the loading control GAPDH (37kDa).

7. Troubleshooting for TLL4 protein expression in MCF-7 cells by ELISA.

To quantify the total TLL4 expression in MCF-7 cells, various attempts to detect the protein by ELISA were performed. The cells were treated differently in order to expose the TLL4 protein for ELISA assessment. Prior to that, the MCF-7 cells were treated with 0nM and 14nM of Paclitaxel for 24hrs. Afterwards, cell samples were extracted with RLT Buffer provided by the RNeasy QIAGEN kit. Another method consists of lysing the cells with either hypotonic KCl solution or Histidine-based lysis buffer. Afterwards, the cells were homogenized using cell-homogenizer.

Lastly, cells were lysed using a water bath ultrasound sonicator. All cell samples were assayed by the human anti-TTLL4 ELISA from MyBioSource and compared to the provided standards (Figure 15); however, the protein was not detectable. All attempts with their specific O.D. readouts are summarized in Table 3.

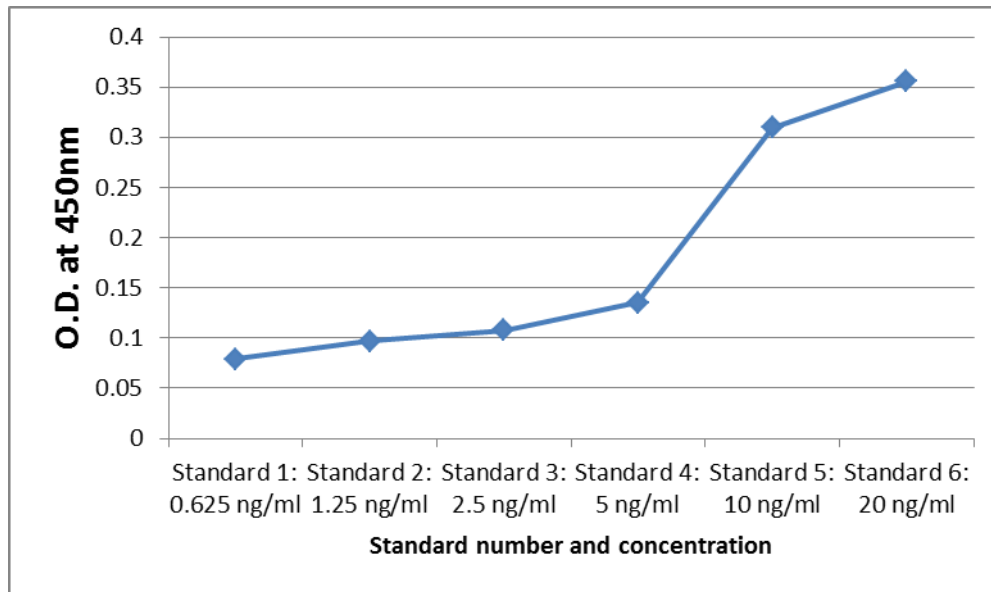


Figure 15: Curve of the O.D. readouts at 450nm for the human anti-TTLL4 ELISA protein standards of concentrations 0.625, 1.25, 2.5, 5, 10 and 20ng/ml.

Method of lysis	Specific information	Blank O.D.	Sample O.D. at 0nM 24hrs	Sample O.D. at 14nM 24hrs
<i>Lysis: RNeasy QIAGEN Buffer</i>	RLT Buffer	0.099	0.063	0.06
<i>Sonication</i>	Cells were dissolved in a solution: 50mM Tris-HCl (pH=7.5) and 1:1000 protease inhibitor cocktail. Then, 15s boost of ultrasound waves with 25s intervals on ice.	0.09	0.059 (only attempted at 0nM)	N/A
<i>Homogenization</i>	Hypotonic solution: 50mM KCl, 1.5mM MgCl ₂ , 10mM Hepes Buffer and 1:1000 protease inhibitor cocktail	0.09	0.079	0.08
	Cell lysis buffer: 150mM Histidine (pH=7.4), 100µl of Triton X100 and 1:1000 protease inhibitor cocktail	0.099	0.068	0.06

Table 3: O.D. readouts of the ELISA troubleshooting attempts to detect and quantify TTLL4 in Paclitaxel treated MCF-7 cells

CHAPTER IV DISCUSSION

TTLL4, a member of the tubulin tyrosine ligase-like family, catalyzes polyglutamylation on various protein substrates including tubulin. TTLL4 was shown to be overexpressed in various types of cancers and may play a role in invasiveness. In this study, we focus on the expression of TTLL4 in breast cancer. Polyglutamylation of tubulin is initiated by TTLL4 resulting in PELP1 transcription factor modulation, which in turn promotes the activation of its substrates including Src, H3, etc. (Kashiwaya et al., 2010). Due to this fact, it was intriguing to examine whether or not TTLL4 expression is altered with Paclitaxel treatment, which targets β -tubulin stabilizing microtubules. Therefore, we hypothesized that TTLL4 expression and/or subcellular localization is altered in breast cancer and that its expression levels decrease cellular sensitivity to the tubulin-targeting chemotherapy drug paclitaxel. It is also possible that TTLL4 expression, subcellular localization &/or enzymatic activity are modulated in response to treatment with Paclitaxel.

It was important to determine the concentrations of Paclitaxel and time points to treat the MCF-7 and MDA-MB-231 cells. The IC_{50} doses for both cell lines were reported in the literature as 220nM for MCF-7 and 320nM for MDA-MB-231 (Constantini et al., 2016 & Motiwala et al., 2015). As such, two suboptimal concentrations were calculated 4-folds below the IC_{50} doses in addition to the 0nM vehicle concentrations of 0.1% DMSO. The four concentrations were initially tested at 24hrs, 2hrs and 30 mins. The counts of living cells showed that the concentrations can be used as IC_{50} doses and suboptimal concentrations in both cell lines despite the slight variation which could be related to some

error in the counting. Nevertheless, after examining the molecular weight of the protein it was best to test the protein levels at 6hrs, 12hrs and 24hrs relating to the time at which the first batch of proteins is produced, the intermediate time, and the time of saturation, respectively. In the same logic the time points for the Real-time PCR experiments were 30 mins, 2hrs and 8hrs.

Our results show that under baseline conditions, expression of *TLL4* normalized to *GAPDH* is significantly elevated in MCF-7 than in MDA-MB-231 cells by 3-fold difference (± 0.15). In order to verify the purity of the TRIzol extraction, RNA from MDA-MB-231 cells were extracted with the QIAGEN RNeasy kit under baseline conditions. The results prove that the extraction by TRIzol was free of contamination due to close Cq values between both extraction methods. The elevated levels of *TLL4* in MCF-7 cells were relevant to the immunofluorescence images, under baseline conditions, which showed higher protein *TLL4* expression in MCF-7 than MDA-MB-231 cells in 2D and 3D images. Furthermore, MCF-7 expresses *TLL4* majorly in the nucleus while *TLL4* in MDA-MB-231 is expressed more in the cytoplasm than in the nucleus. Therefore, the MCF-7 cell line might need the higher pool of *TLL4* in order to express more of the protein and as such transduce signals that would lead to transformation for enhanced survival and invasiveness. This could be the reason why *TLL4* protein is located mainly in the nucleus of MCF-7 cells affecting gene expression, transcription, and translation (Kashiwaya et al., 2010). Nevertheless, the expression of *TLL4* in MDA-MB-231 is evident.

As for the Western Blot results, the difference in the expression of *TLL4* under baseline conditions between MCF-7 and MDA-MB-231 cells is not decipherable. *TLL4* is

made up of 10 isoforms and contains many phosphorylation sites in addition to other post-translation modifications; this leads to the appearance of various bands making it difficult to discern the difference in *TLL4* expression between the cell lines. The different bands also appear in wild-type MEFs; thus, this property is not restricted to the breast cancer cell lines. The Western Blot data provide an insight into the complex structure of the *TLL4* enzyme.

Moreover, since it was difficult to assess the expression by Western Blot, *TLL4* was attempted to be quantified by means of ELISA. However, *TLL4* was not detectable by the ELISA kit despite many troubleshooting of cell lysis procedures. This may be because of a problem with the kit itself.

As mentioned in the hypothesis, *TLL4* expression may be altered by Paclitaxel treatment or may alter the response of the cells to Paclitaxel. The RTPCR results post-Paclitaxel treatment of MCF-7 cells show no significant difference in *TLL4* expression between the various Paclitaxel concentrations and the control, and between the different time points. Nevertheless, the expression of *TLL4* increases upon Paclitaxel treatment (55nM and 220nM Paclitaxel at 30 mins and 2hrs; 14nM Paclitaxel at 8hrs; and 220nM Paclitaxel at 8hrs). At the protein level, the immunofluorescence 2D and 3D images show an increased expression of *TLL4* majorly after 24hrs of treatment in all treatment concentrations. However, the increased expression is also evident in 55nM and 220nM concentrations at 6hrs and 12hrs. The increased *TLL4* expression caused by an increase in *TLL4* pools in MCF-7 cells could be the result of stabilized microtubules that require more polyglutamylation. The results may also suggest that the increased *TLL4* expression would cause a signaling cascade conferring expression of genes related to growth,

proliferation and resistance for the better survival of the cancer cells. To be more specific, the elevated expression of *TTL4* increases the polyglutamylation of PELP1 and NAP protein. PELP1 would activate Src, and p85 of PI3K, and affect histone acetylation. NAP proteins would modulate histones and affect gene transcription (Kashiwaya et al., 2010 & Janke et al., 2008). It is to be regarded that the expression of *TTL4* is observed in the cells that survive the Paclitaxel treatment. The Western Blot data does not give a clear perception of the expression of *TTL4* in MCF-7 cells after Paclitaxel treatment. Although not quantifiable, the western blots show the expression of two isoforms: majorly the isoform of molecular weight 27kDa and a faint band of that of molecular weight 23kDa. Additionally, thicker bands were visualized in 220nM Paclitaxel at 6hrs, 55nM at 12hrs and 24hrs, and 14nM at 24hrs which reflect some of the immunofluorescence data. Nevertheless, the blots require more optimization in order to allow a clearer representation of all bands and possibly more isoforms of the enzyme.

On the other hand, *TTL4* expression was assessed in MDA-MB-231 cells post Paclitaxel treatment. The Paclitaxel treatment for MDA-MB-231 cells was performed in a similar fashion as for the MCF-7 cells but with concentrations of 0nM, 20nM, 80nM and 320nM. The RTPCR data suggest that there is no significant change in the expression of *TTL4* upon treatment with Paclitaxel yet there is variation in the gene's mean fold change. At 20nM Paclitaxel treatment, *TTL4* levels decrease as compared to the 0nM control at all time points. At 80nM Paclitaxel treatment, *TTL4* levels increase at all time points as compared to the control. At 320nM Paclitaxel treatment, *TTL4* levels, when compared to the vehicle, increase at 30 mins and 8hrs of treatment but slightly decrease at 2hrs of the treatment. With regards to *TTL4* protein levels, immunofluorescence results show

increased expression in 20nM, 80nM and 320nM concentrations as compared to the 0nM vehicle. However, at all time points, 320nM Paclitaxel treatment shows the highest *TLL4* expression. The immunofluorescence data may suggest that *TLL4* is expressed at higher concentrations upon treatment with Paclitaxel in order to promote polyglutamylation of downstream signaling molecules allowing for survival and resistance gene expression (Kashiwaya et al., 2010). *TLL4* may also affect Paclitaxel's binding to tubulin molecules and conferring cell resistance via PI3K signaling and sonic hedgehog pathways (Kashiwaya et al., 2010 & Sangrajrang & Fellous, 2000). Furthermore, the 320nM Paclitaxel treatment images may consist of the cells that resisted the treatment by overexpressing *TLL4* or overexpress *TLL4* and influence Paclitaxel's binding. The combined RTPCR and immunofluorescence data represent the protein's variation in expression levels in response to Paclitaxel treatment.

In conclusion, this pilot study provides an insight into the role that *TLL4* may play in breast cancer. At the protein level, *TLL4* is a complex molecule made of various isoforms and includes multiple sites for post-translational modifications. According to the CCLE, *TLL4* is overexpressed in breast cancer cells. Our data indicate MCF-7 cells express higher levels of *TLL4* as compared to MDA-MB-231 cells. In response to Paclitaxel treatment, *TLL4* may affect downstream signaling molecules resulting in cell survival or resistance. Moreover, *TLL4* may influence Paclitaxel's mode of action and microtubule stabilizing role.

In the future, it would be advantageous to determine *TLL4* expression in MCF10A cells by RTPCR and immunofluorescence in order to compare the results obtained in MCF-7 and MDA-MB-231 cells. We further need to optimize current protein quantification

methods including Western Blot – by adding complete phosphatase inhibitor cocktails – and/or ELISA – through designing an ELISA kit that detects TTLL4. The immunofluorescence images are to be scored to determine the expression levels of TTLL4 more accurately. In addition, we should examine whether or not Paclitaxel affects the activity of TTLL4 – if it affects the substrates of TTLL4: tubulin and NAP1/2. Furthermore, to determine the essentiality of TTLL4, we could knock down or knock out *TTLL4* and assess cell survival and resistance under baseline conditions and post-Paclitaxel treatment.

Ultimately, learning more about TTLL4 and its role in cancer would provide information about cell survival and cell resistance mechanisms used by cancer cells in response to chemotherapeutic treatment. Additionally, because TTLL4 is a target of novel immunotherapies (Nakamura et al., 2013), elucidating new data about TTLL4 offers better understanding of its essentiality, mechanism of action, substrates, etc.

CHAPTER V

REFERENCES

- Aken, B.L., Ayling, S., Barrell, D., Clarke, L., Curwen, V., Fairley, S., Banet, J.F., Billis, K., Girón, C.G., Hourlier, T., Howe, K., Kähäri, A., Kokocinski, F., Martin, F.J., Murphy, D.N., Nag, R., Ruffier, M., Schuster, M., Tang, Y.A., Vogel, J.H., White, S., Zadissa, A., Flicek, P. & Searle, S.M.J. The Ensembl gene annotation system. Database 2016, baw093 [doi: 10.1093/database/baw093](https://doi.org/10.1093/database/baw093).
- Audebert, S., Desbruyeres, E., Gruszczynski, C., Koulakoff, A., Gros, F., Denoulet, P. & Edde, B. (1993). Reversible Polyglutamylation of α - and β -Tubulin and Microtubule Dynamics in Mouse Brain Neurons. *Molecular Biology of the Cell*, 4: 615-626.
- Barbuti, A.M. & Chen, Z.S. (2015). Paclitaxel through the ages of anticancer therapy: Exploring its role in chemoresistance and radiation therapy. *Cancers*, 7, 2360-2371.
- Becker, S. (2015). A historic and scientific review of breast cancer: The next global healthcare challenge. *International Journal of Gynecology and Obstetrics*, 131, S36-S39.
- Berchem G.J., Bosseler M., Mine N., Avalosse B. (1999). Nanomolar range docetaxel treatment sensitizes MCF-7 cells to chemotherapy induced apoptosis, induces G2M arrest and phosphorylates bcl-2. *Anticancer Res.* 19(1A):535–40.

- Bernard-Marty, C., Treilleux, I., Dumontet, C., Cardoso, F., Fellous, A., Gancberg, D., Bissery, M.C., Paesmans, M., Larsimont, D., Piccart, M.J. & Di Leo, A. (2002). Microtubule-associated parameters as predictive markers of docetaxel activity in advanced breast cancer patients: Results of a pilot study. *Clinical Breast Cancer*, 3(5), 341-345.
- Cell Signaling Technology, Inc. (n.d.). Protein Page: TLL4 (human). Retrieved February 14, 2017, from <http://www.phosphosite.org/proteinAction?id=21452&showAllSites=true#appletMsg>
- Costantini, D.L., Villani, D. F., Vallis, K. A. & Reilly, R. M. (2016). Methotrexate, Paclitaxel, and Doxorubicin Radiosensitize HER2-Amplified Human Breast Cancer Cells to the Auger Electron–Emitting Radiotherapeutic Agent ¹¹¹In-NLS-Trastuzumab. *The Journal Of Nuclear Medicine*, 51(3), 477-483.
- Dai, X., Li, T., Bai, Z., Yang, Y., Liu, X., Zhan, J. & Shi, B. (2015). Breast cancer intrinsic subtype classification, clinical use and future trends. *American Journal for Cancer Research*, 5(10), 2929-2943.
- Froidevaux-Klipfel, L., Targa, B., Cantaloube, I., Ahmed-Zaid, H., Poüs, C. & Baillet, A. (2015). Septin cooperation with tubulin polyglutamylation contributes to cancer cell adaptation to taxanes. *Oncotarget*, 6(34): 36063-36080.
- Garnham, C., Vemu, A., Wilson-Kubalek, E., Yu, I., Szyk, A., Lander, G., Milligan, R. & Roll-Mecak, A. (2015). Multivalent microtubule recognition

by Tubulin Tyrosine Ligase-Like family Glutamylases. *Cell*, 161(5), 1112-1123.

Ibrado A.M., Kim C.N., Bhalla K. (1998). Temporal relationship of CDK1 activation and mitotic arrest to cytosolic accumulation of cytochrome C and caspase-3 activity during Taxol-induced apoptosis of human AML HL-60 cells. *Leukemia*. 12(12):1930–6.

Ijaz, F., Hatanaka, Y., Hatanaka, T., Tsutsumi, K., Iwaki, T., Umemura, K., Ikegami, K., & Setou M. (2016). Proper cytoskeletal architecture beneath the plasma membrane of red blood cells requires Ttl4. *Molecular Biological Cell*.

Inman, J.L., Robertson, C., Mott, J.D. & Bissel, M.J. (2015). Mammary gland development: cell fate specification, stem cells and the microenvironment. *Development*, 142(6), 1028-1042.

Janke, C. (2014). The tubulin code: Molecular components, readout mechanisms, and functions. *Journal of Cell Biology*, 206(4), 461–472. doi: 0.1083/jcb.201406055

Janke, C., Rogowski, K. & van Dijk, J. (2008). Polyglutamylation: a fine-regulator of protein function? *EMBO Reports*, 9(7), 636-641.

Kashiwaya, K., Nakagawa, H., Hosokawa, M., Ueda, Y.M.K., Piao, L., Chung, S., Hamamoto, R., Eguchi, H., Ohigashi, H., Ishikawa, O., Janke, C., Shinomura, Y. & Nakamura, Y. (2010). Involvement of the Tubulin Tyrosine Ligase-Like family member 4 (TTLL4) in PELP1

- polyglutamylation and chromatin remodeling in pancreatic cancer cells. *Cancer Research*, 70(10), 4024-4033.
- Kingston, D. (2001). Taxol, a molecule for all seasons. *Chemical Communications*, (10), 867-880.
- Lanigan, F. O'Conner, D., Martin, F. & Gallagher, W.M. (2007). Molecular links between mammary gland development and breast cancer. *Cellular and Molecular Life Sciences: CMLS*, 64(24), 3159-3184.
- Ling Y.H., Consoli U., Tornos C., Andreeff M., Perez-Soler R. (1998). Accumulation of cyclin B1, activation of cyclin B1-dependent kinase and induction of programmed cell death in human epidermoid carcinoma KB cells treated with taxol. *Int J Cancer*. 75(6):925–32.
- Makki, J. (2015). Diversity of breast carcinoma: Histological subtypes and clinical relevance. *Clinical Medicine Insights: Pathology*, 8, 23-31.
- Motiwala, M.N. & Rangari, V. D. (2015). Combined effect of paclitaxel and piperine on a MCF-7 breast cancer cell line in vitro: Evidence of a synergistic interaction. *Synergy*, 2, 1-6.
- Murray, S., Briasoulis, E., Linardou, H., Badaloukos, D. & Papadimitriou, C. (2012). Taxane resistance in breast cancer: Mechanisms, predictive biomarkers and circumvention strategies. *Cancer Treatment Reviews*, 38, 890-903.
- Nakamura, Y., Tsunoda, T. & Osawa, R. (2013). United States Patent No.
- Nelso, C. M & Gjorevski, N. (2011). Integrated morphodynamic signaling of the mammary gland. *Nature Reviews Molecular Cell Biology*, 12.

- Orr, G., Verdier-Pinard, P., McDaid, H. & Horwitz, S.B. (2003). Mechanisms of Taxol resistance related to microtubules. *Oncogene*, 22(47), 7280-7295.
- Rao, S., Horwitz, S.B. & Ringel, I. (1992). Direct photoaffinity labeling of tubulin with taxol. *J. Natl. Cancer Inst.*, 84: 785–788.
- Robinson, G. W. (2007). Cooperation of signalling pathways in embryonic mammary gland development. *Nat Rev Genet*, 8(12), 963-972.
- Sangrajang S. & Fellous A.. (2000). Taxol Resistance. *Chemotherapy*, 46, 327-334.
- Sun, X., Park, J. H., Gumerson, J., Wu, Z., Swaroop, A., Qian, H., Roll-Mecak, A. & Li, T. (2015). Loss of RGPR glutamylation underlies the pathogenic mechanism of retinal dystrophy caused by TLL5 mutations. *PNAS*, E2925-E2934.
- Van Dijk, J., Miro, J., Strub, J.M., Lacroix, B., van Dorsselaer, A., Edde, B. & Janke, C. (2008). Polyglutamylation is a post-translational modification with a broad range of substrates. *The Journal of Biological Chemistry*, 283(7), 3915-3922.
- Van Dijk, J., Rogowski, K., Miro, J., Lacroix, B., Edde, B. & Janke, C. (2007). A targeted multienzyme mechanism for selective microtubule polyglutamylation. *Molecular Cell*, 26, 437-448.
- Wang S., Wang Z., Boise L., Dent P., Grant S. (199). Loss of the bcl-2 phosphorylation loop domain increases resistance of human leukemia cells (U937) to paclitaxel-mediated mitochondrial dysfunction and apoptosis. *Biochem Biophys Res Commun*. 259(1):67–72.

- Wasylyk, C., Zambrano, A., Zhao, C., Brants, J., Abecassis, J., Schalken, J., Rogatsch, H., Schaefer, G., Pycha, A. & Wasylyk, H.K.B. (2010). Tubulin tyrosine ligase like 12 links to prostate cancer through tubulin posttranslational modification and chromosome ploidy. *International Journal of Cancer*, 127, 2542-2553.
- Watson, C.J. & Khaled, W.T. (2008). Mammary development in the embryo and adult; a journey of morphogenesis and commitment. *Development*, 135(6), 995-1003.
- Wysolmerski, J. & Cowin, P. (2010). Molecular mechanisms guiding embryonic mammary gland development. *Cold Spring Harbor Perspectives in Biology*, 2(6).
- Ye, B., Li, C., Yang, Z., Wang, Y., Hao, J., Wang, L., Li, Y., Du, Y., Hao, L., Liu, B., Wang, S., Xia, P., Huang, G., Sub, L., Tian, Y. & Fan, Z. (2014). Cytosolic carboxypeptidase CCP6 is required for megakaryopoiesis by modulating Mad2 polyglutamylation. *The Journal of Experimental Medicine*, 211(12), 2439-2454.
- Yuan J., Kramer A., Matthes Y., Yan R., Spankuch B., Gatje R., et al. (2006). Stable gene silencing of cyclin B1 in tumor cells increases susceptibility to taxol and leads to growth arrest in vivo. *Oncogene*. 25(12):1753–62.